

## Construction of a 21-Component Layered Mixture Experiment Design

G. F. Piepel  
S. K. Cooley  
B. Jones \*

\* SAS Institute Inc.

September, 2004



Prepared for the U.S. Department of Energy  
under Contract DE-AC06-76RL01830

---

## DISCLAIMER

This report was prepared as an account of work sponsored by an agency of the United States Government. Neither the United States Government nor any agency thereof, nor Battelle Memorial Institute, nor any of their employees, makes **any warranty, express or implied, or assumes any legal liability or responsibility for the accuracy, completeness, or usefulness of any information, apparatus, product, or process disclosed, or represents that its use would not infringe privately owned rights.** Reference herein to any specific commercial product, process, or service by trade name, trademark, manufacturer, or otherwise does not necessarily constitute or imply its endorsement, recommendation, or favoring by the United States Government or any agency thereof, or Battelle Memorial Institute. The views and opinions of authors expressed herein do not necessarily state or reflect those of the United States Government or any agency thereof.

PACIFIC NORTHWEST NATIONAL LABORATORY  
*operated by*  
BATTELLE  
*for the*  
UNITED STATES DEPARTMENT OF ENERGY  
*under Contract DE-AC06-76RL01830*



This document was printed on recycled paper.

## **Construction of a 21-Component Layered Mixture Experiment Design**

G. F. Piepel  
S. K. Cooley  
B. Jones \*

\*SAS Institute Inc

September 2004  
(Previously Cleared as PNNL-SA-37340, Rev. 0, October 2002)

Prepared for  
the U.S. Department of Energy  
under Contract DE-AC06-76RL01830

Pacific Northwest National Laboratory  
Richland, Washington 99352

## Abstract

This paper describes the solution to a unique and challenging mixture experiment design problem involving: 1) 19 and 21 components for two different parts of the design, 2) many single-component and multi-component constraints, 3) augmentation of existing data, 4) a layered design developed in stages, and 5) a no-candidate-point optimal design approach. The problem involved studying the liquidus temperature of spinel crystals as a function of nuclear waste glass composition. The statistical objective was to develop an experimental design by augmenting existing glasses with new nonradioactive and radioactive glasses chosen to cover the designated nonradioactive and radioactive experimental regions.

The existing 144 glasses were expressed as 19-component nonradioactive compositions and then augmented with 40 new nonradioactive glasses. These included 8 glasses on the outer layer of the region, 27 glasses on an inner layer, 2 replicate glasses at the centroid, and one replicate each of three existing glasses. Then, the  $144 + 40 = 184$  glasses were expressed as 21-component radioactive compositions and augmented with 5 radioactive glasses. A D-optimal design algorithm was used to select the new outer layer, inner layer, and radioactive glasses.

Several statistical software packages can generate D-optimal experimental designs, but nearly all require a set of candidate points (e.g., vertices) from which to select design points. The large number of components (19 or 21) and many constraints made it impossible to generate the huge number of vertices and other typical candidate points. JMP® was used to select design points without candidate points. JMP uses a coordinate-exchange algorithm modified for mixture experiments, which is discussed in the paper.

## Acknowledgments

We thank John Vienna, the glass scientist and project manager at Pacific Northwest National Laboratory (PNNL) responsible for the spinel  $T_L$  study. He contributed significantly to planning the work discussed in this paper. We also acknowledge the input of David Peeler, Tommy Edwards, and Kevin Brown from Westinghouse Savannah River Company. They supplied several useful comments in planning the spinel  $T_L$  study. We acknowledge Steve Lambert from Numatec Hanford Company for supporting the liquidus temperature research. We also thank Bill Holtzscheiter from the Tanks Focus Area (Immobilization Technology Integration Manager) for his support of the project that included the spinel  $T_L$  study. Finally, we acknowledge Alejandro Heredia-Langner and Andrea Currie of PNNL for respectively performing technical and editorial reviews of the paper.

We also especially thank SAS Institute Inc. for allowing Bradley Jones to make custom modifications to a post-Version 4 development version of JMP, provide that software, and perform software test runs. These efforts allowed developing the new spinel  $T_L$  experimental design in the short time frame required.

The work of Greg Piepel and Scott Cooley was funded by the U.S. Department of Energy Office of Science and Technology under the Tanks Focus Area. Their work was performed at the Pacific Northwest National Laboratory, which is operated for the U.S. Department of Energy by Battelle under Contract DE-AC06-76RL01830.

# Contents

|   |     |
|---|-----|
| Abstract .....  | iii |
| Acknowledgments.....  | iv  |
| 1.0 Introduction.....   | 1   |
| 2.0 Background of Waste Glass Example.....  | 2   |
| 3.0 Construction of the Layered Design for Spinel Liquidus Temperature .....        | 3   |
| 4.0 Summary .....   | 13  |
| 5.0 References.....   | 14  |
| Appendix A, Candidate Set Free Approach to D-Optimal Mixture Design .....           | A.1 |
| Appendix B, Existing Glass Compositions Augmented by New Design .....               | B.1 |
| Appendix C, Dot Plots for Existing Glasses and New Experimental Design Glasses..... | C.1 |

## Tables

|     |  |     |
|-----|--|-----|
| 1   | Single-Component Constraints on the Original and Normalized Mass Fractions of the 21 Components Varied in Studying Spinel TL of HLW Glasses .....                                      | 5   |
| 2   | Multi-Component Constraints(a) on the Normalized Mass Fractions of the 21 Components Varied in Studying Spinel TL of HLW Glasses .....   | 6   |
| 3   | Expanded(a) Single-Component Constraints on the Normalized Mass Fractions of 19 Components Used to Determine the Existing Glasses Augmented with New Experimental Design Glasses ..... | 7   |
| 4   | Un-normalized 22-Component Mass-Fraction Compositions of the 45 Experimental Design Glasses for the Spinel TL Study .....  | 10  |
| B.1 | Un-normalized 22-Component Mass-Fraction Compositions of the 144 Existing Database Glasses in the Spinel Primary Phase Field Chosen for Augmentation.....                              | B.7 |

## Figure

|     |  |          |
|-----|--|----------|
| C.1 | Dot Plots of 21-Component Normalized Mass Fractions for 144 Existing Spinel Glasses and 45 New Experimental Design Glasses ..... | C.2-C.12 |
|-----|--|----------|

# 1.0 Introduction

This paper describes the unique and challenging construction of a constrained mixture experiment design for a nuclear waste glass application. In general, a constrained mixture experiment involves varying the proportions of two or more mixture components within specified constraints and then measuring one or more response variables of interest for every mixture. In a mixture experiment, the proportions of the components must lie between zero and one, and sum to 1 for every mixture. In constrained mixture experiments, there are additional constraints consisting of lower and/or upper bounds on: 1) single components (single-component constraints) and/or 2) linear combinations of components (multi-component constraints). Cornell (2002) provides a comprehensive discussion of the design and analysis of mixture experiments.

The nuclear waste glass application discussed in this paper involved studying the liquidus temperature ( $T_L$ ) of spinel crystals as a function of glass composition. The statistical objective was to develop a constrained mixture experiment design that augments existing glasses with 40 new nonradioactive glasses and 5 new radioactive glasses. The new glasses were to be chosen from designated nonradioactive and radioactive experimental regions using a *layered design* approach (Piepel et al. 1993, 2002). A layered design contains points on the boundary of the experimental region (designated the *outer layer*), points on one or more interior layers of the experimental region (designated the *inner layers*), and a center point and replicates if desired. For the spinel  $T_L$  layered design, only one inner layer was used. The outer and inner layers of the nonradioactive and radioactive experimental regions were defined by single-component and multi-component constraints involving 19 nonradioactive components and 2 radioactive components. Hence, the layers of the nonradioactive experimental region were defined by constraints on 19 glass components, while the layers of the radioactive experimental region were defined by constraints on 21 glass components.

The typical approach for constructing constrained mixture experiment designs is to use software to generate a set of candidate design points covering the experimental region and then use optimal experimental design software to select a subset of the candidate points. Candidate points usually include at least the vertices, and possibly other boundary points, of the constrained region.

The typical design construction approach could not be used for the spinel  $T_L$  experimental design. The plan had been to use the vertices of the outer and inner layers of the nonradioactive and radioactive experimental regions as candidate points to construct the layered design. However, there were too many vertices for the MIXSOFT software (Piepel 1999) to generate and store, due to the large numbers of components and constraints. Assigning most of the computer's unused hard disk space to extended memory (to store vertices during the generation process) was not enough to resolve the problem. Ideas for generating a fraction of the vertices from which an optimal design could be selected (analogous to the work of Piepel (1990, 1991) but accounting for the multi-component constraints) were pursued, but were not successful due to the high dimensionality of the problem. Ultimately, a customized version of a no-candidate optimal design capability in JMP® (2000) was used to generate the spinel  $T_L$  layered design.

The following section of the paper provides some background information on the need to design an experiment to augment existing waste glass compositions with new waste glass compositions in the spinel primary phase field. The subsequent section of the paper discusses the steps used to construct the spinel  $T_L$  layered design. The paper closes with a brief summary section. Appendix A discusses and illustrates the JMP capability to generate designs without candidate points. Appendix B lists the existing glass compositions that were augmented by the new experimental design discussed in this paper. Appendix C includes a graphical comparison of the existing and new glass compositions.



## 2.0 Background of Waste Glass Example

The Hanford Site in southeastern Washington State has 177 underground waste tanks containing 204,400 m<sup>3</sup> of wastes generated from more than four decades of nuclear fuel processing and actinide separations (Kirkbride 2000). These wastes will be retrieved from the tanks, separated into high-level waste (HLW) and low-activity waste (LAW) fractions, and separately vitrified (i.e., made into waste glass). HLW glass is the focus of the study addressed in this paper.

Models that relate waste glass properties to composition play important roles in retrieving and vitrifying HLW. Property-composition models are useful for: 1) estimating the volume of HLW glass that will be produced, 2) optimizing glass compositions, and 3) judging the impacts of changes in waste compositions, blending scenarios, and pretreatment scenarios. Property-composition models will also be used to control the HLW vitrification process and demonstrate that the waste glass satisfies applicable requirements and constraints.

Developing suitable HLW glass property-composition models is an iterative process. Interim models are used to project the appropriate glass composition regions and predict values of the key or limiting glass properties to be modeled as functions of glass compositions. Experimental data then are generated to improve estimates of the key glass properties in composition regions of interest and the model development process is repeated. With this iterative process, composition regions are continually updated and property models improved.

Calculations have shown that the constraint on the liquidus temperature ( $T_L$ ) property will limit the waste loading in nearly all Hanford HLW glasses. The  $T_L$  constraint often is taken as the absence of solid inclusions in the melt at a nominal temperature. However, an alternative constraint is to limit solid inclusions to a small, fixed crystal fraction (e.g., 1 volume percent) at a nominal temperature. One of the primary phase fields of concern is spinel, which has the general formula  $(\text{Ni,Fe,Mn})(\text{Cr,Fe})_2\text{O}_4$ . Property-composition models are required to implement the spinel  $T_L$  constraints. Hence, data are required to develop the models.

A glass composition –  $T_L$  database for more than 200 glasses in the spinel primary phase field is reported by Vienna et al. (2001) and Jiricka et al. (2001). However, only some of these data are applicable for Hanford HLW glasses. This paper discusses the steps of the experimental design process used to select new HLW glass compositions to augment existing glass compositions within the spinel primary phase field of the expected Hanford HLW glass composition region.

### 3.0 Construction of the Layered Design for Spinel Liquidus Temperature

A statistical experimental design approach was used to develop new HLW glass compositions to augment existing spinel  $T_L$  data for 144 glass compositions relevant to Hanford HLW. A layered design approach for mixture experiments (Piepel et al. 1993, 2002) was used to select an additional 40 glasses (including 4 replicates) not containing uranium ( $U_3O_8$ ) and thorium ( $ThO_2$ ). Then, an additional 5 glasses containing  $U_3O_8$  and  $ThO_2$  were selected. The specific steps used to implement this approach are described in this section.

#### Step 1: Define the HLW Glass Composition Experimental Region

Glass scientists applied glass formulation methods to the best available estimates of Hanford HLW compositions to project possible waste glass compositions. They then selected 21 HLW glass components ( $Al_2O_3$ ,  $B_2O_3$ ,  $Bi_2O_3$ ,  $CaO$ ,  $CdO$ ,  $Cr_2O_3$ ,  $F$ ,  $Fe_2O_3$ ,  $K_2O$ ,  $Li_2O$ ,  $MnO$ ,  $Na_2O$ ,  $NiO$ ,  $P_2O_5$ ,  $SiO_2$ ,  $SrO$ ,  $ThO_2$ ,  $TiO_2$ ,  $U_3O_8$ ,  $ZnO$ ,  $ZrO_2$ ) whose effects on spinel  $T_L$  were to be investigated. Included in the 21 components were two radioactive components,  $U_3O_8$  and  $ThO_2$ . Single-component and multi-component constraints on the mass fractions of these 21 glass components were specified to define the experimental glass composition region. A twenty-second component—"Others", a mixture of the remaining minor waste components—was held constant at a mass-fraction value of 0.015 for all new glasses tested.

Denoting the mass fraction of glass component  $i$  by  $X_i$ , the applicable single-component constraints on the 22 components were of the form

$$0 \leq L_i \leq X_i \leq U_i < 1 \text{ for } i = 1, 2, \dots, 21 \quad \text{and} \quad X_{22} = 0.015, \quad (1)$$

and the mixture constraints were of the form

$$\sum_{i=1}^{21} X_i = 0.985 \quad \text{and} \quad \sum_{i=1}^{22} X_i = 1. \quad (2)$$

In addition to the constraints in Equations (1) and (2), constraints on glass properties were implemented using modifications of linear mixture models developed during previous studies. These linear mixture models were of the form

$$\hat{y} = \sum_{i=1}^{22} b_i X_i, \quad (3)$$

where  $\hat{y}$  was the fitted property (or appropriate mathematical transformation thereof), the  $b_i$  were fitted model coefficients, and the  $X_i$  were mass fractions of the 22 glass components that sum to 1 as in Equation (2). Multi-component constraints based on linear mixture models of the form in Equation (3) were written in the general form

$$\sum_{i=1}^{22} A_i X_i + A_0 \geq 0, \quad (4)$$

where the  $A_i$ ,  $i = 1, 2, \dots, 22$  were coefficients (or their negatives) from the linear mixture models, and  $A_0$  was obtained from the limiting value for a property.

The spinel  $T_L$  experimental design was not constructed in terms of the 22 components. Rather, the design was constructed using normalized mass fractions of: 1) the 19 components varied in the nonradioactive portion of the design, and 2) the 21 components varied in the radioactive portion of the design. Normalized mass fractions for the 19 nonradioactive components were defined as

$$g_i = \frac{X_i}{\sum_{i=1}^{19} X_i}, i = 1, 2, \dots, 19 \quad \text{where} \quad \sum_{i=1}^{19} g_i = 1, \quad (5)$$

with  $i = 1, 2, \dots, 19$  denoting the nonradioactive components. Similarly, normalized mass fractions for the 21 glass components (including  $U_3O_8$  and  $ThO_2$ , but excluding Others) were defined as

$$x_i = \frac{X_i}{\sum_{i=1}^{21} X_i}, i = 1, 2, \dots, 21 \quad \text{where} \quad \sum_{i=1}^{21} x_i = 1, \quad (6)$$

with  $i = 1, 2, \dots, 21$  denoting the 21 components listed previously. In Equations (5) and (6), the  $X_i$  satisfy the constraints in Equations (1), (2), and (4). For all glasses in the new experimental design,

$\sum_{i=1}^{21} X_i = 0.985$ . However, this sum took different values for glasses in the existing database. For existing glasses as well as new experimental design glasses, the sum of the normalized mass fractions  $g_i$  (for 19 components) and  $x_i$  (for 21 components) was 1, as shown in Equations (5) and (6).

The outer and inner layers of the HLW glass composition experimental region were defined by lower and upper bounds on the normalized 21-component mass fractions  $x_i$ , as well as lower and/or upper bounds on glass properties (implemented by preliminary linear mixture models). The lower and upper bounds on the  $x_i$  were denoted by

$$0 \leq l_i \leq x_i \leq u_i < 1 \quad \text{for} \quad i = 1, 2, \dots, 21 \quad \text{where} \quad l_i = \frac{L_i}{0.985} \quad \text{and} \quad u_i = \frac{U_i}{0.985}. \quad (7)$$

The multi-component constraints on the  $x_i$  were obtained by re-expressing the multi-component constraints on the  $X_i$  [from Equation (4)] as follows:

$$\begin{aligned} \sum_{i=1}^{21} A_i X_i + A_{Others} X_{Others} + A_0 &\geq 0 \\ \sum_{i=1}^{21} (0.985 A_i) \left( \frac{X_i}{0.985} \right) + A_{Others} (0.015) + A_0 &\geq 0 \\ \sum_{i=1}^{21} a_i x_i + a_0 &\geq 0 \quad \text{where} \quad a_i = 0.985 A_i \quad \text{and} \quad a_0 = A_{Others} (0.015) + A_0. \end{aligned} \quad (8)$$

Single-component constraints of the form in Equation (7) used to define the outer and inner layers of the experimental region are summarized in Table 1. Multi-component constraints of the form in Equation (8) used to define the outer and inner layers are summarized in Table 2. Note that both outer and inner layers are defined for nonradioactive glasses (without  $U_3O_8$  and  $ThO_2$ ), but that only an inner layer region is defined for radioactive glasses (containing  $U_3O_8$  and/or  $ThO_2$ ). Thus, the single-component constraints on  $U_3O_8$  and  $ThO_2$  are summarized under the “Inner Layer” columns of Table 1. The lower and upper

Table 1. Single-Component Constraints on the Original and Normalized Mass Fractions of the 21 Components Varied in Studying Spinel  $T_L$  of HLW Glasses

| HLW Glass Component                          | Outer Layer                 |          |                             |          | Inner Layer                 |          |                             |          |
|--|-----------------------------|----------|-----------------------------|----------|-----------------------------|----------|-----------------------------|----------|
|  | Lower Limit (mass fraction) |          | Upper Limit (mass fraction) |          | Lower Limit (mass fraction) |          | Upper Limit (mass fraction) |          |
|  | Orig. <sup>(a)</sup>        | Norm.    | Orig.                       | Norm.    | Orig.                       | Norm.    | Orig.                       | Norm.    |
| Al <sub>2</sub> O <sub>3</sub>               | 0.025                       | 0.025381 | 0.15                        | 0.152284 | 0.06                        | 0.060914 | 0.10                        | 0.101523 |
| B <sub>2</sub> O <sub>3</sub>                | 0.03                        | 0.030457 | 0.20                        | 0.203046 | 0.05                        | 0.050761 | 0.12                        | 0.121827 |
| Bi <sub>2</sub> O <sub>3</sub>               | 0                           | 0        | 0.07                        | 0.071066 | 0                           | 0        | 0.05                        | 0.050761 |
| CaO  | 0                           | 0        | 0.03                        | 0.030457 | 0                           | 0        | 0.02                        | 0.020305 |
| CdO  | 0                           | 0        | 0.02                        | 0.020305 | 0                           | 0        | 0.01                        | 0.010152 |
| Cr <sub>2</sub> O <sub>3</sub>               | 0                           | 0        | 0.012                       | 0.012183 | 0.003                       | 0.003046 | 0.008                       | 0.008122 |
| F  | 0                           | 0        | 0.02                        | 0.020305 | 0.005                       | 0.005076 | 0.015                       | 0.015228 |
| Fe <sub>2</sub> O <sub>3</sub>               | 0.03                        | 0.030457 | 0.20                        | 0.203046 | 0.07                        | 0.071066 | 0.14                        | 0.142132 |
| K <sub>2</sub> O                             | 0                           | 0        | 0.06                        | 0.060914 | 0.015                       | 0.015228 | 0.045                       | 0.045685 |
| Li <sub>2</sub> O                            | 0                           | 0        | 0.06                        | 0.060914 | 0.015                       | 0.015228 | 0.045                       | 0.045685 |
| MnO  | 0                           | 0        | 0.06                        | 0.060914 | 0.01                        | 0.010152 | 0.03                        | 0.030457 |
| Na <sub>2</sub> O                            | 0.10                        | 0.101523 | 0.20                        | 0.203046 | 0.125                       | 0.126904 | 0.175                       | 0.177665 |
| NiO  | 0.003                       | 0.003046 | 0.03                        | 0.030457 | 0.005                       | 0.005076 | 0.02                        | 0.020305 |
| P <sub>2</sub> O <sub>5</sub>                | 0                           | 0        | 0.025                       | 0.025381 | 0.005                       | 0.005076 | 0.0125                      | 0.012690 |
| SiO <sub>2</sub>                             | 0.28                        | 0.284264 | 0.50                        | 0.507614 | 0.34                        | 0.345178 | 0.46                        | 0.467005 |
| SrO  | 0                           | 0        | 0.04                        | 0.040609 | 0                           | 0        | 0.02                        | 0.020305 |
| ThO <sub>2</sub> <sup>(b)</sup>              | 0                           | 0        | 0                           | 0        | 0.005                       | 0.005076 | 0.02                        | 0.020305 |
| TiO <sub>2</sub>                             | 0                           | 0        | 0.04                        | 0.040609 | 0                           | 0        | 0.02                        | 0.020305 |
| U <sub>3</sub> O <sub>8</sub> <sup>(b)</sup> | 0                           | 0        | 0                           | 0        | 0.02                        | 0.020305 | 0.08                        | 0.081218 |
| ZnO  | 0                           | 0        | 0.02                        | 0.020305 | 0                           | 0        | 0.02                        | 0.020305 |
| ZrO <sub>2</sub>                             | 0                           | 0        | 0.08                        | 0.081218 | 0.01                        | 0.010152 | 0.03                        | 0.030457 |

- (a) “Orig.” denotes the original 22-component mass fraction basis of glass composition, while “Norm.” denotes the 21-component normalized mass fraction basis.
- (b) ThO<sub>2</sub> and U<sub>3</sub>O<sub>8</sub> were not involved in defining the outer or inner layers of the nonradioactive glass composition region of interest. The lower and upper limits listed for ThO<sub>2</sub> and U<sub>3</sub>O<sub>8</sub> are listed in the inner layer columns because the radioactive glasses were selected from the glass composition region defined by the inner layer constraints on the remaining 19 components.

limits on U<sub>3</sub>O<sub>8</sub>, ThO<sub>2</sub>, and the remaining 19 components were used to define the radioactive (inner layer) glass composition region to be studied.

Six glass property constraints, implemented via preliminary linear mixture models, are listed in Table 2. The first two property constraints in Table 2 correspond to  $800^{\circ}\text{C} \leq T_L \leq 1300^{\circ}\text{C}$ . Spinel  $T_L$  values below at least  $1050^{\circ}\text{C}$  were considered desirable. However, data for glasses with larger spinel  $T_L$  values were also needed so property-composition models to be developed from the data will adequately predict acceptable as well as unacceptable values. The third and fourth property constraints in Table 2 correspond to  $950^{\circ}\text{C} \leq T_5 \leq 1250^{\circ}\text{C}$ , where  $T_5$  is the temperature at which the viscosity of glass is 5 Pa-s. These constraints limited attention to glasses with desirable viscosities within the range of the operating and idling temperatures for glass melters. Finally, the last two property constraints in Table 2 were intended to ensure that elemental releases of B and Na from glass subjected to the Product Consistency Test (PCT) leach test (ASTM 1998) would be below  $6 \text{ g/m}^2$ . It is relatively easy to make HLW glasses

with these PCT releases below 1.0 or even 0.5 g/m<sup>2</sup>. However, specifications for HLW glass allow larger values in the neighborhood of 6 g/m<sup>2</sup>. Hence, these larger limits were used so that glasses with larger as well as smaller PCT releases were included in the experimental region.

## Step 2: Screen the Existing Database for Glasses in the Composition Region of Interest

Because the goal was to augment relevant existing spinel T<sub>L</sub>-composition data with new data, the existing data were screened to determine the glasses having compositions within the composition region defined by the outer layer constraints in Table 1 and the multi-component constraints in Table 2. However, an insufficient number of glass compositions were obtained, so the single-component constraints in Table 1 were expanded to those shown in Table 3. Generally, the lower and upper limits on

Table 2. Multi-Component Constraints<sup>(a)</sup> on the Normalized Mass Fractions of the 21 Components Varied in Studying Spinel T<sub>L</sub> of HLW Glasses

| HLW Glass Component                          | Outer and Inner Layers |                         |                        |                         |  |   |
|--|------------------------|-------------------------|------------------------|-------------------------|--|---|
|  | 800°C ≤ T <sub>L</sub> | T <sub>L</sub> ≤ 1300°C | 950°C ≤ T <sub>S</sub> | T <sub>S</sub> ≤ 1250°C | r <sub>B</sub> <sup>PCT</sup> ≤ 6 g/m <sup>2</sup> | r <sub>Na</sub> <sup>PCT</sup> ≤ 6 g/m <sup>2</sup> |
| Al <sub>2</sub> O <sub>3</sub>               | 2935.300               | -2935.300               | 15942.268              | -14730.718              | 25.0609  | 25.2382   |
| B <sub>2</sub> O <sub>3</sub>                | 299.440                | -299.440                | -5769.433              | 9817.782                | -11.6531   | -9.2329   |
| Bi <sub>2</sub> O <sub>3</sub>               | 3160.865               | -3160.865               | 2173.186               | 2850.314                | -0.1619  | 0.7900  |
| CaO  | 2129.570               | -2129.570               | -6292.227              | 13029.627               | 8.9104   | 2.0062  |
| CdO  | 2689.050               | -2689.050               | 2173.186               | 2850.314                | -0.1619  | 0.7900  |
| Cr <sub>2</sub> O <sub>3</sub>               | 20722.430              | -20722.430              | 2173.186               | 2850.314                | -0.1619  | 0.7900  |
| F  | 3160.865               | -3160.865               | 2173.186               | 2850.314                | -0.1619  | 0.7900  |
| Fe <sub>2</sub> O <sub>3</sub>               | 2689.050               | -2689.050               | 957.199                | 934.001                 | 3.0544   | 4.0509  |
| K <sub>2</sub> O                             | -700.335               | 700.335                 | -12748.201             | 15585.001               | -17.5586   | -19.4127  |
| Li <sub>2</sub> O                            | -1563.195              | 1563.195                | -47087.157             | 48416.907               | -22.6252   | -19.5352  |
| MnO  | 943.630                | -943.630                | 2173.186               | 2850.314                | -0.1619  | 0.7900  |
| Na <sub>2</sub> O                            | -1629.190              | 1629.190                | -12748.201             | 15585.001               | -17.5586   | -19.4127  |
| NiO  | 9092.535               | -9092.535               | 2173.186               | 2850.314                | -0.1619  | 0.7900  |
| P <sub>2</sub> O <sub>5</sub>                | 3160.865               | -3160.865               | 2173.186               | 2850.314                | -0.1619  | 0.7900  |
| SiO <sub>2</sub>                             | 978.105                | -978.105                | 14699.080              | -11419.030              | 4.2386   | 4.4037  |
| SrO  | 2129.570               | -2129.570               | -6292.227              | 13029.627               | 8.9104   | 2.0062  |
| ThO <sub>2</sub> <sup>(b)</sup>              | 3160.865               | -3160.865               | 16070.370              | -6921.220               | 10.4704  | 11.4313   |
| TiO <sub>2</sub>                             | 5280.585               | -5280.585               | 2173.186               | 2850.314                | -0.1619  | 0.7900  |
| U <sub>3</sub> O <sub>8</sub> <sup>(b)</sup> | 1422.340               | -1422.340               | 2173.186               | 2850.314                | -0.1619  | 0.7900  |
| ZnO  | 2689.050               | -2689.050               | 2173.186               | 2850.314                | -0.1619  | 0.7900  |
| ZrO <sub>2</sub>                             | 3160.865               | -3160.865               | 16070.366              | -6821.216               | 10.4704  | 11.4313   |
| Constant                                     | -751.865               | 1251.865                | -1935.506              | 2494.837                | 1.7893   | 1.8038  |

- (a) The multi-component constraints are of the form shown in the last line of Equation (8). In this table, the component names represent the  $a_i$  coefficients and “Constant” represents the  $a_0$  coefficient. The coefficients of the constraints have been rounded to the shown number of decimal places.
- (b) The ThO<sub>2</sub> and U<sub>3</sub>O<sub>8</sub> constraint terms were used only to define the normalized 21-component glass composition region including both nonradioactive and radioactive components. The ThO<sub>2</sub> and U<sub>3</sub>O<sub>8</sub> constraint terms were not used to define the normalized 19-component nonradioactive glass composition region.

each component were extended by 10% of their values in Table 1, although for NiO the lower limit was set to 0. The following sub-steps were used to screen the existing data.

- For each glass in the existing database, the normalized mass fractions of the 19 nonradioactive components were calculated using the formula in Equation (5). With this procedure,  $U_3O_8$  was removed from the normalized compositions of glasses containing it. This was judged reasonable based on the assumption that  $U_3O_8$  does not affect spinel  $T_L$ . Hence, with this approach, glasses containing  $U_3O_8$  were considered in selecting nonradioactive glasses.
- All glasses in the existing database not satisfying the normalized single-component constraints in Table 3 were eliminated.
- All glasses in the existing database not satisfying the normalized multi-component constraints in Table 2 were eliminated.

The initial database contained  $T_L$  values for 214 glasses in the spinel primary-phase field. After the glass compositions were screened according to the preceding sub-steps, 144 glass compositions remained. Table B.1 of Appendix B lists these 144 glass compositions, expressed in un-normalized mass fractions of the 22 components discussed in Step 1.

Table 3. Expanded<sup>(a)</sup> Single-Component Constraints on the Normalized Mass Fractions of 19 Components Used to Determine the Existing Glasses Augmented with New Experimental Design Glasses

| Waste Glass Component | Lower Limit (mass fraction) | Upper Limit (mass fraction) |
|-----------------------|-----------------------------|-----------------------------|
| $Al_2O_3$             | 0.025381                    | 0.152284                    |
| $B_2O_3$              | 0.030457                    | 0.203046                    |
| $Bi_2O_3$             | 0                           | 0.071066                    |
| $CaO$                 | 0                           | 0.030457                    |
| $CdO$                 | 0                           | 0.020305                    |
| $Cr_2O_3$             | 0                           | 0.012183                    |
| F                     | 0                           | 0.020305                    |
| $Fe_2O_3$             | 0.030457                    | 0.203046                    |
| $K_2O$                | 0                           | 0.060914                    |
| $Li_2O$               | 0                           | 0.060914                    |
| $MnO$                 | 0                           | 0.060914                    |
| $Na_2O$               | 0.101523                    | 0.203046                    |
| $NiO$                 | 0.003046                    | 0.030457                    |
| $P_2O_5$              | 0                           | 0.025381                    |
| $SiO_2$               | 0.284264                    | 0.507614                    |
| $SrO$                 | 0                           | 0.040609                    |
| $ThO_2$               | (b)                         | (b)                         |
| $TiO_2$               | 0                           | 0.040609                    |
| $U_3O_8$              | (b)                         | (b)                         |
| $ZnO$                 | 0                           | 0.020305                    |
| $ZrO_2$               | 0                           | 0.081218                    |

(a) For most components, the lower and upper bounds from Table 1 were expanded by 10%.

(b)  $U_3O_8$  and  $ThO_2$  were not used to screen the existing glasses. However, none of the existing glasses contained  $ThO_2$ . Some glasses did contain  $U_3O_8$ , but none would have been screened out by the  $U_3O_8$  upper limit. Thus, there was no impact from using normalized 19-component compositions to screen existing data.

### Step 3: Assess Screened Existing Data

As mentioned previously, the strategy called for selecting 40 new glasses without  $U_3O_8$  and  $ThO_2$ , then selecting 5 new glasses containing  $U_3O_8$  and/or  $ThO_2$ . The 40 and 5 glasses were selected to augment the screened existing data. Of the 144 glasses satisfying the constraints in Tables 2 and 3, 130 glasses did not contain  $U_3O_8$  and 14 did contain  $U_3O_8$ . None of the existing glasses in the spinel  $T_L$  database contained  $ThO_2$ .

The 144 screened, existing glasses were graphically assessed with dot plots (Figure C.1 in Appendix C) to assess how well the glasses covered the glass component ranges of interest. The existing data spanned ranges of some components fairly well. For other components ( $B_2O_3$ ,  $Cr_2O_3$ , F,  $K_2O$ ,  $MnO$ ,  $P_2O_5$ ,  $SrO$ ,  $TiO_2$ , and  $ZnO$ ), there were limited data for larger values within component ranges. None of the existing glasses contained  $Bi_2O_3$  or  $ThO_2$ . It was concluded that the 144 screened existing glasses provided reasonable support for augmenting with new glasses, but that the new glasses would have to fill in uncovered or inadequately covered portions of the HLW glass composition experimental region.

#### **Step 4: Augment Screened Existing Glasses with Outer-Layer Glasses (No $U_3O_8$ and $ThO_2$ )**

At this step, the objective was to construct a constrained mixture experiment design for 19 components, excluding  $U_3O_8$  and  $ThO_2$ . The 144 screened, existing glass compositions were expressed as normalized mass fractions of the 19 components calculated according to Equation (5). The 14 glasses containing  $U_3O_8$  were included in these 144 glasses, so  $U_3O_8$  was removed from the normalized compositions. Assuming that  $U_3O_8$  will not affect spinel  $T_L$ , the 14  $U_3O_8$  glasses were retained in the set of normalized 19-component compositions to be augmented. These 14 glasses did not contain  $ThO_2$ , so  $ThO_2$  was not removed in the normalized 19-component compositions. The remaining  $144 - 14 = 130$  glasses did not contain  $U_3O_8$  or  $ThO_2$ , so their normalized 19-component compositions were the same as their normalized 21-component compositions.

A total of 8 distinct outer-layer glasses were selected to optimally augment the 144 screened existing glasses, expressed as normalized 19-component compositions. Only 8 glasses were selected from the outer layer because outer-layer compositions are less likely to be produced from Hanford HLW.

A customized, post-Version 4 development version of JMP (2000) was obtained courtesy of Dr. Brad Jones of SAS Institute Inc. to perform the optimal augmentation. JMP can optimally generate or augment existing data with new data points without having to select from a set of candidate design points. This capability is discussed and illustrated in Appendix A. The traditional approach of generating all of the extreme vertices of the outer layer to use as candidate design points for optimal experimental design software was attempted first. However, this approach was unsuccessful because of the inability of existing software [e.g., MIXSOFT (1999)] and computers to generate and store the extremely large number of vertices. So, the “augment design” capability of JMP was used to D-optimally augment the existing 144 glasses with 8 new glasses on the outer layer composition region defined in Tables 1 and 2. A linear mixture model of the form

$$\text{Spinel } T_L = \sum_{i=1}^{19} \beta_i x_i \quad (9)$$

in the 19 normalized components was used to implement the D-optimal criterion in JMP.

#### **Step 5: Augment Existing Screened Glasses + Outer-Layer Glasses with Inner-Layer Glasses (No $U_3O_8$ and $ThO_2$ )**

At this step, 27 inner-layer glasses were selected to augment the 144 screened, existing glasses and the 8 outer-layer glasses selected in Step 4. The inner layer was defined by the single-component constraints in the “Inner Layer” columns of Table 1 and by the multi-component constraints in Table 2 (which apply to both the outer and inner layers). The customized, development version of JMP mentioned in Step 4 was used to select the 27 inner-layer compositions to D-optimally augment the  $144 + 8 = 152$  existing and new glasses. Again, a linear mixture model of the form in Equation (9) was assumed.

Steps 4 and 5 were performed several times, which provided several candidate designs of 8 + 27 new glass compositions. Dot plots and scatterplot matrices were used to compare how well the candidate designs covered the glass composition experimental region. The preliminary property-composition models used to define the multi-component constraints in Table 2 were used to predict glass property values for the points in each candidate design. Dot plots and scatterplot matrices then were used to assess how well each candidate design covered glass property ranges and regions. Based on these graphical comparisons of candidate designs, the set of 8 + 27 = 35 compositions judged the best was selected for use.

Although the 8 outer layer and 27 inner layer glasses were selected based on 19-component normalized compositions, for completeness they are listed in Table 4 as 22-component compositions. The 8 outer-layer glasses are listed as SPA-1 to SPA-8, and the 27 inner-layer compositions are listed as SPA-9 to SPA-35. The 19-component normalized compositions may be calculated from the 22-component compositions in Table 4 using the formula in Equation (5).

#### **Step 6: Add Overall Centroid and Replicates to the Experimental Design**

A center glass composition (for the nonradioactive glass composition region) was calculated by averaging the 8 outer-layer and 27 inner-layer compositions and added to the experimental design. Traditionally, a center glass composition is calculated by averaging all extreme vertices of the composition region of interest (e.g., the outer and/or inner layers). However, there were too many vertices to generate them with existing software, as previously discussed. Hence, it was decided to average the selected 8 outer-layer and 27 inner-layer glasses to form a center glass in the nonradioactive composition region. The center glass composition and replicates were chosen without  $\text{U}_3\text{O}_8$  and  $\text{ThO}_2$  because of the desire to limit (to 5) the number of radioactive glasses melted and tested.

Four replicates also were added to the experimental design to provide for assessing experimental and property measurement variation. Replicates of the center glass (SPA-36) and three existing glasses (SP-1, SG-18, and LSi-Al-16) were selected to span the composition and property spaces. In Table 4, the center glass composition is denoted SPA-36 and the replicate compositions are denoted SPA-37 to SPA-40.

#### **Step 7: Augment Existing Nonradioactive and Radioactive Glasses and New Nonradioactive Glasses with New Radioactive Glasses**

Steps 4, 5, and 6 focused on selecting the 40 experimental design glasses without  $\text{U}_3\text{O}_8$  and  $\text{ThO}_2$ . The compositions of those glasses were expressed as normalized mass fractions of 19 components, which also may be thought of as normalized mass fractions of 21 components with  $\text{U}_3\text{O}_8 = 0$  and  $\text{ThO}_2 = 0$ .

In this step, the 144 screened existing glasses (14 with  $\text{U}_3\text{O}_8$ ) and the 40 newly selected nonradioactive glasses were augmented with 5 new radioactive glasses (containing  $\text{U}_3\text{O}_8$  and  $\text{ThO}_2$ ). The existing 144 + new 40 glasses were expressed in normalized mass fractions of the 21 components, according to Equation (6). The 5 radioactive glasses were selected within a glass composition region defined by the inner-layer single-component constraints in Table 1 and the multi-component constraints in Table 2.

The customized version of JMP (previously discussed) was used to select the 5 radioactive glasses. A linear mixture model in the 21 normalized components was assumed. Again, several alternative sets of 5 radioactive glasses were generated using JMP, and one set was selected based on graphical assessments of how well the 5 radioactive compositions were spread over glass composition and glass property spaces. The selected 5 radioactive compositions are listed as glasses SPA-41 to SPA-45 in Table 4.



Table 4. Un-normalized 22-Component Mass-Fraction Compositions of the 45 Experimental Design Glasses for the Spinel  $T_L$  Study

| Waste Glass Component          | Glass <sup>(a)</sup> |        |        |        |        |        |        |        |        |        |        |        |
|--------------------------------|----------------------|--------|--------|--------|--------|--------|--------|--------|--------|--------|--------|--------|
|                                | SPA-01               | SPA-02 | SPA-03 | SPA-04 | SPA-05 | SPA-06 | SPA-07 | SPA-08 | SPA-09 | SPA-10 | SPA-11 | SPA-12 |
| Al <sub>2</sub> O <sub>3</sub> | 0.0765               | 0.1475 | 0.1500 | 0.0928 | 0.0541 | 0.0702 | 0.1281 | 0.0676 | 0.1000 | 0.1000 | 0.1000 | 0.1000 |
| B <sub>2</sub> O <sub>3</sub>  | 0.1505               | 0.1235 | 0.1139 | 0.1019 | 0.1904 | 0.0703 | 0.1511 | 0.1690 | 0.0872 | 0.0500 | 0.0825 | 0.0814 |
| Bi <sub>2</sub> O <sub>3</sub> | 0.0700               | 0.0000 | 0.0420 | 0.0160 | 0.0000 | 0.0700 | 0.0000 | 0.0700 | 0.0000 | 0.0500 | 0.0491 | 0.0000 |
| CaO                            | 0.0000               | 0.0033 | 0.0000 | 0.0000 | 0.0300 | 0.0300 | 0.0300 | 0.0300 | 0.0200 | 0.0000 | 0.0000 | 0.0200 |
| CdO                            | 0.0000               | 0.0200 | 0.0000 | 0.0000 | 0.0000 | 0.0200 | 0.0200 | 0.0200 | 0.0000 | 0.0000 | 0.0000 | 0.0000 |
| Cr <sub>2</sub> O <sub>3</sub> | 0.0070               | 0.0000 | 0.0000 | 0.0000 | 0.0021 | 0.0009 | 0.0120 | 0.0000 | 0.0080 | 0.0080 | 0.0030 | 0.0080 |
| F                              | 0.0000               | 0.0200 | 0.0200 | 0.0000 | 0.0200 | 0.0200 | 0.0200 | 0.0000 | 0.0050 | 0.0050 | 0.0150 | 0.0150 |
| Fe <sub>2</sub> O <sub>3</sub> | 0.1031               | 0.1324 | 0.1213 | 0.1514 | 0.0300 | 0.0467 | 0.0917 | 0.0450 | 0.1259 | 0.1373 | 0.1345 | 0.1096 |
| K <sub>2</sub> O               | 0.0315               | 0.0556 | 0.0000 | 0.0600 | 0.0499 | 0.0600 | 0.0003 | 0.0032 | 0.0150 | 0.0327 | 0.0150 | 0.0150 |
| Li <sub>2</sub> O              | 0.0015               | 0.0000 | 0.0292 | 0.0000 | 0.0000 | 0.0497 | 0.0397 | 0.0333 | 0.0450 | 0.0327 | 0.0185 | 0.0255 |
| MnO                            | 0.0501               | 0.0367 | 0.0000 | 0.0000 | 0.0600 | 0.0000 | 0.0189 | 0.0600 | 0.0300 | 0.0187 | 0.0300 | 0.0267 |
| Na <sub>2</sub> O              | 0.1170               | 0.1094 | 0.1343 | 0.1215 | 0.1000 | 0.1000 | 0.1458 | 0.1000 | 0.1379 | 0.1376 | 0.1281 | 0.1598 |
| NiO                            | 0.0126               | 0.0030 | 0.0049 | 0.0030 | 0.0247 | 0.0030 | 0.0030 | 0.0030 | 0.0050 | 0.0050 | 0.0050 | 0.0171 |
| P <sub>2</sub> O <sub>5</sub>  | 0.0000               | 0.0217 | 0.0000 | 0.0250 | 0.0250 | 0.0250 | 0.0000 | 0.0250 | 0.0125 | 0.0125 | 0.0050 | 0.0050 |
| SiO <sub>2</sub>               | 0.3565               | 0.2924 | 0.3694 | 0.3324 | 0.2820 | 0.2981 | 0.2837 | 0.2800 | 0.3435 | 0.3834 | 0.3693 | 0.3769 |
| SrO                            | 0.0000               | 0.0000 | 0.0000 | 0.0400 | 0.0400 | 0.0400 | 0.0061 | 0.0000 | 0.0200 | 0.0022 | 0.0000 | 0.0000 |
| ThO <sub>2</sub>               | 0.0000               | 0.0000 | 0.0000 | 0.0000 | 0.0000 | 0.0000 | 0.0000 | 0.0000 | 0.0000 | 0.0000 | 0.0000 | 0.0000 |
| TiO <sub>2</sub>               | 0.0000               | 0.0121 | 0.0000 | 0.0209 | 0.0000 | 0.0012 | 0.0000 | 0.0305 | 0.0200 | 0.0000 | 0.0000 | 0.0150 |
| U <sub>3</sub> O <sub>8</sub>  | 0.0000               | 0.0000 | 0.0000 | 0.0000 | 0.0000 | 0.0000 | 0.0000 | 0.0000 | 0.0000 | 0.0000 | 0.0000 | 0.0000 |
| ZnO                            | 0.0086               | 0.0074 | 0.0000 | 0.0200 | 0.0000 | 0.0000 | 0.0200 | 0.0200 | 0.0000 | 0.0000 | 0.0200 | 0.0000 |
| ZrO <sub>2</sub>               | 0.0000               | 0.0000 | 0.0000 | 0.0000 | 0.0768 | 0.0800 | 0.0146 | 0.0283 | 0.0100 | 0.0100 | 0.0100 | 0.0100 |
| Others                         | 0.0150               | 0.0150 | 0.0150 | 0.0150 | 0.0150 | 0.0150 | 0.0150 | 0.0150 | 0.0150 | 0.0150 | 0.0150 | 0.0150 |

| Waste Glass Component          | Glass <sup>(a)</sup> |        |        |        |        |        |        |        |        |        |        |        |
|--------------------------------|----------------------|--------|--------|--------|--------|--------|--------|--------|--------|--------|--------|--------|
|                                | SPA-13               | SPA-14 | SPA-15 | SPA-16 | SPA-17 | SPA-18 | SPA-19 | SPA-20 | SPA-21 | SPA-22 | SPA-23 | SPA-24 |
| Al <sub>2</sub> O <sub>3</sub> | 0.1000               | 0.0600 | 0.1000 | 0.0600 | 0.0600 | 0.0600 | 0.0882 | 0.1000 | 0.0690 | 0.0600 | 0.1000 | 0.1000 |
| B <sub>2</sub> O <sub>3</sub>  | 0.0953               | 0.0500 | 0.0500 | 0.0500 | 0.1169 | 0.0818 | 0.0657 | 0.0500 | 0.0673 | 0.0971 | 0.0500 | 0.0500 |
| Bi <sub>2</sub> O <sub>3</sub> | 0.0000               | 0.0000 | 0.0500 | 0.0500 | 0.0000 | 0.0000 | 0.0382 | 0.0020 | 0.0500 | 0.0286 | 0.0500 | 0.0500 |
| CaO                            | 0.0000               | 0.0200 | 0.0000 | 0.0000 | 0.0000 | 0.0200 | 0.0164 | 0.0200 | 0.0200 | 0.0000 | 0.0000 | 0.0200 |
| CdO                            | 0.0000               | 0.0000 | 0.0100 | 0.0100 | 0.0100 | 0.0000 | 0.0000 | 0.0100 | 0.0100 | 0.0100 | 0.0000 | 0.0000 |
| Cr <sub>2</sub> O <sub>3</sub> | 0.0080               | 0.0030 | 0.0077 | 0.0080 | 0.0030 | 0.0030 | 0.0030 | 0.0080 | 0.0075 | 0.0030 | 0.0080 | 0.0030 |
| F                              | 0.0150               | 0.0150 | 0.0150 | 0.0150 | 0.0150 | 0.0150 | 0.0150 | 0.0150 | 0.0050 | 0.0150 | 0.0050 | 0.0050 |
| Fe <sub>2</sub> O <sub>3</sub> | 0.1167               | 0.1400 | 0.1400 | 0.0700 | 0.0744 | 0.1400 | 0.0732 | 0.0846 | 0.0991 | 0.0756 | 0.0700 | 0.0820 |
| K <sub>2</sub> O               | 0.0150               | 0.0150 | 0.0226 | 0.0150 | 0.0450 | 0.0389 | 0.0150 | 0.0450 | 0.0450 | 0.0450 | 0.0450 | 0.0450 |
| Li <sub>2</sub> O              | 0.0428               | 0.0450 | 0.0450 | 0.0150 | 0.0150 | 0.0379 | 0.0450 | 0.0450 | 0.0160 | 0.0391 | 0.0450 | 0.0450 |
| MnO                            | 0.0244               | 0.0300 | 0.0300 | 0.0300 | 0.0100 | 0.0100 | 0.0300 | 0.0300 | 0.0300 | 0.0100 | 0.0300 | 0.0100 |
| Na <sub>2</sub> O              | 0.1564               | 0.1681 | 0.1472 | 0.1480 | 0.1647 | 0.1589 | 0.1708 | 0.1293 | 0.1250 | 0.1511 | 0.1750 | 0.1750 |
| NiO                            | 0.0159               | 0.0200 | 0.0050 | 0.0133 | 0.0200 | 0.0050 | 0.0150 | 0.0050 | 0.0050 | 0.0146 | 0.0200 | 0.0050 |
| P <sub>2</sub> O <sub>5</sub>  | 0.0122               | 0.0125 | 0.0125 | 0.0125 | 0.0050 | 0.0050 | 0.0050 | 0.0050 | 0.0050 | 0.0050 | 0.0125 | 0.0050 |
| SiO <sub>2</sub>               | 0.3584               | 0.3400 | 0.3400 | 0.4600 | 0.3760 | 0.3554 | 0.3681 | 0.3661 | 0.3835 | 0.3922 | 0.3445 | 0.3400 |
| SrO                            | 0.0000               | 0.0000 | 0.0000 | 0.0183 | 0.0000 | 0.0142 | 0.0084 | 0.0200 | 0.0000 | 0.0000 | 0.0000 | 0.0000 |
| ThO <sub>2</sub>               | 0.0000               | 0.0000 | 0.0000 | 0.0000 | 0.0000 | 0.0000 | 0.0000 | 0.0000 | 0.0000 | 0.0000 | 0.0000 | 0.0000 |
| TiO <sub>2</sub>               | 0.0149               | 0.0200 | 0.0000 | 0.0000 | 0.0200 | 0.0000 | 0.0000 | 0.0200 | 0.0000 | 0.0088 | 0.0200 | 0.0200 |
| U <sub>3</sub> O <sub>8</sub>  | 0.0000               | 0.0000 | 0.0000 | 0.0000 | 0.0000 | 0.0000 | 0.0000 | 0.0000 | 0.0000 | 0.0000 | 0.0000 | 0.0000 |
| ZnO                            | 0.0000               | 0.0200 | 0.0000 | 0.0000 | 0.0200 | 0.0099 | 0.0180 | 0.0000 | 0.0200 | 0.0000 | 0.0000 | 0.0000 |
| ZrO <sub>2</sub>               | 0.0100               | 0.0264 | 0.0100 | 0.0100 | 0.0300 | 0.0300 | 0.0100 | 0.0300 | 0.0276 | 0.0300 | 0.0100 | 0.0300 |
| Others                         | 0.0150               | 0.0150 | 0.0150 | 0.0150 | 0.0150 | 0.0150 | 0.0150 | 0.0150 | 0.0150 | 0.0150 | 0.0150 | 0.0150 |

(a) SPA-1 to SPA-8 are outer-layer glasses, SPA-9 to SPA-35 are inner-layer glasses, SPA-36 is a center point, SPA-37 to SPA-40 are replicates (see text discussion), and SPA-41 to SPA-45 are radioactive glasses.

Table 4. Un-normalized 22-Component Mass-Fraction Compositions of the 45 Experimental Design Glasses for the Spinel T<sub>L</sub> Study (cont.)

| Waste Glass Component          | Glass <sup>(a)</sup> |        |        |        |        |        |        |        |        |        |        |        |
|--------------------------------|----------------------|--------|--------|--------|--------|--------|--------|--------|--------|--------|--------|--------|
|                                | SPA-25               | SPA-26 | SPA-27 | SPA-28 | SPA-29 | SPA-30 | SPA-31 | SPA-32 | SPA-33 | SPA-34 | SPA-35 | SPA-36 |
| Al <sub>2</sub> O <sub>3</sub> | 0.1000               | 0.1000 | 0.0642 | 0.1000 | 0.0613 | 0.0600 | 0.0966 | 0.0605 | 0.0633 | 0.0600 | 0.0799 | 0.0729 |
| B <sub>2</sub> O <sub>3</sub>  | 0.0500               | 0.0793 | 0.1200 | 0.0556 | 0.0968 | 0.1200 | 0.0500 | 0.1009 | 0.1200 | 0.0644 | 0.1200 | 0.0952 |
| Bi <sub>2</sub> O <sub>3</sub> | 0.0000               | 0.0000 | 0.0500 | 0.0000 | 0.0500 | 0.0500 | 0.0483 | 0.0000 | 0.0500 | 0.0000 | 0.0000 | 0.0268 |
| CaO                            | 0.0000               | 0.0200 | 0.0000 | 0.0046 | 0.0200 | 0.0200 | 0.0000 | 0.0000 | 0.0200 | 0.0200 | 0.0000 | 0.0115 |
| CdO                            | 0.0000               | 0.0000 | 0.0000 | 0.0100 | 0.0000 | 0.0000 | 0.0000 | 0.0000 | 0.0100 | 0.0100 | 0.0100 | 0.0077 |
| Cr <sub>2</sub> O <sub>3</sub> | 0.0057               | 0.0080 | 0.0080 | 0.0080 | 0.0080 | 0.0080 | 0.0030 | 0.0030 | 0.0073 | 0.0080 | 0.0080 | 0.0046 |
| F                              | 0.0150               | 0.0150 | 0.0050 | 0.0050 | 0.0050 | 0.0050 | 0.0150 | 0.0150 | 0.0150 | 0.0050 | 0.0150 | 0.0077 |
| Fe <sub>2</sub> O <sub>3</sub> | 0.1237               | 0.0721 | 0.0700 | 0.1400 | 0.1293 | 0.1144 | 0.1376 | 0.0700 | 0.1377 | 0.1138 | 0.0700 | 0.0952 |
| K <sub>2</sub> O               | 0.0150               | 0.0450 | 0.0450 | 0.0450 | 0.0150 | 0.0276 | 0.0150 | 0.0450 | 0.0150 | 0.0450 | 0.0450 | 0.0230 |
| Li <sub>2</sub> O              | 0.0150               | 0.0434 | 0.0150 | 0.0450 | 0.0450 | 0.0150 | 0.0393 | 0.0150 | 0.0150 | 0.0450 | 0.0229 | 0.0230 |
| MnO                            | 0.0300               | 0.0100 | 0.0100 | 0.0300 | 0.0100 | 0.0100 | 0.0100 | 0.0300 | 0.0300 | 0.0300 | 0.0100 | 0.0230 |
| Na <sub>2</sub> O              | 0.1274               | 0.1661 | 0.1644 | 0.1250 | 0.1280 | 0.1626 | 0.1593 | 0.1750 | 0.1326 | 0.1435 | 0.1702 | 0.1383 |
| NiO                            | 0.0050               | 0.0050 | 0.0050 | 0.0050 | 0.0097 | 0.0144 | 0.0112 | 0.0050 | 0.0050 | 0.0200 | 0.0050 | 0.0134 |
| P <sub>2</sub> O <sub>5</sub>  | 0.0125               | 0.0050 | 0.0050 | 0.0125 | 0.0050 | 0.0050 | 0.0104 | 0.0125 | 0.0050 | 0.0125 | 0.0050 | 0.0096 |
| SiO <sub>2</sub>               | 0.4357               | 0.3447 | 0.3734 | 0.3447 | 0.3576 | 0.3487 | 0.3592 | 0.4227 | 0.3475 | 0.3516 | 0.3619 | 0.3644 |
| SrO                            | 0.0200               | 0.0200 | 0.0200 | 0.0046 | 0.0200 | 0.0000 | 0.0200 | 0.0000 | 0.0016 | 0.0038 | 0.0200 | 0.0154 |
| ThO <sub>2</sub>               | 0.0000               | 0.0000 | 0.0000 | 0.0000 | 0.0000 | 0.0000 | 0.0000 | 0.0000 | 0.0000 | 0.0000 | 0.0000 | 0.0000 |
| TiO <sub>2</sub>               | 0.0000               | 0.0134 | 0.0200 | 0.0000 | 0.0000 | 0.0000 | 0.0000 | 0.0000 | 0.0000 | 0.0025 | 0.0121 | 0.0154 |
| U <sub>3</sub> O <sub>8</sub>  | 0.0000               | 0.0000 | 0.0000 | 0.0000 | 0.0000 | 0.0000 | 0.0000 | 0.0000 | 0.0000 | 0.0000 | 0.0000 | 0.0000 |
| ZnO                            | 0.0200               | 0.0079 | 0.0000 | 0.0200 | 0.0143 | 0.0143 | 0.0000 | 0.0200 | 0.0000 | 0.0200 | 0.0200 | 0.0077 |
| ZrO <sub>2</sub>               | 0.0100               | 0.0300 | 0.0100 | 0.0300 | 0.0100 | 0.0100 | 0.0100 | 0.0104 | 0.0100 | 0.0300 | 0.0100 | 0.0306 |
| Others                         | 0.0150               | 0.0150 | 0.0150 | 0.0150 | 0.0150 | 0.0150 | 0.0150 | 0.0150 | 0.0150 | 0.0150 | 0.0150 | 0.0150 |

| Waste Glass Component          | Glass <sup>(a)</sup> |        |        |        |        |        |        |        |        |  |  |  |
|--------------------------------|----------------------|--------|--------|--------|--------|--------|--------|--------|--------|--|--|--|
|                                | SPA-37               | SPA-38 | SPA-39 | SPA-40 | SPA-41 | SPA-42 | SPA-43 | SPA-44 | SPA-45 |  |  |  |
| Al <sub>2</sub> O <sub>3</sub> | 0.0729               | 0.0800 | 0.0250 | 0.1600 | 0.1000 | 0.0632 | 0.0600 | 0.0600 | 0.0669 |  |  |  |
| B <sub>2</sub> O <sub>3</sub>  | 0.0952               | 0.0700 | 0.0999 | 0.0560 | 0.1006 | 0.0818 | 0.0500 | 0.1195 | 0.0500 |  |  |  |
| Bi <sub>2</sub> O <sub>3</sub> | 0.0268               | 0.0000 | 0.0000 | 0.0000 | 0.0000 | 0.0500 | 0.0000 | 0.0000 | 0.0500 |  |  |  |
| CaO                            | 0.0115               | 0.0100 | 0.0030 | 0.0010 | 0.0000 | 0.0000 | 0.0000 | 0.0037 | 0.0200 |  |  |  |
| CdO                            | 0.0077               | 0.0070 | 0.0000 | 0.0153 | 0.0100 | 0.0100 | 0.0000 | 0.0000 | 0.0100 |  |  |  |
| Cr <sub>2</sub> O <sub>3</sub> | 0.0046               | 0.0022 | 0.0030 | 0.0012 | 0.0080 | 0.0073 | 0.0080 | 0.0080 | 0.0030 |  |  |  |
| F                              | 0.0077               | 0.0006 | 0.0000 | 0.0001 | 0.0150 | 0.0150 | 0.0050 | 0.0050 | 0.0150 |  |  |  |
| Fe <sub>2</sub> O <sub>3</sub> | 0.0952               | 0.1250 | 0.1499 | 0.1356 | 0.0794 | 0.0732 | 0.0949 | 0.1117 | 0.0750 |  |  |  |
| K <sub>2</sub> O               | 0.0230               | 0.0028 | 0.0150 | 0.0003 | 0.0450 | 0.0150 | 0.0193 | 0.0450 | 0.0150 |  |  |  |
| Li <sub>2</sub> O              | 0.0230               | 0.0300 | 0.0599 | 0.0140 | 0.0150 | 0.0450 | 0.0196 | 0.0150 | 0.0437 |  |  |  |
| MnO                            | 0.0230               | 0.0036 | 0.0300 | 0.0116 | 0.0100 | 0.0100 | 0.0300 | 0.0146 | 0.0100 |  |  |  |
| Na <sub>2</sub> O              | 0.1383               | 0.1573 | 0.1099 | 0.2100 | 0.1250 | 0.1278 | 0.1547 | 0.1750 | 0.1639 |  |  |  |
| NiO                            | 0.0134               | 0.0052 | 0.0005 | 0.0087 | 0.0200 | 0.0135 | 0.0050 | 0.0050 | 0.0166 |  |  |  |
| P <sub>2</sub> O <sub>5</sub>  | 0.0096               | 0.0046 | 0.0000 | 0.0028 | 0.0125 | 0.0050 | 0.0125 | 0.0125 | 0.0050 |  |  |  |
| SiO <sub>2</sub>               | 0.3644               | 0.4600 | 0.4921 | 0.3394 | 0.4073 | 0.4008 | 0.3400 | 0.3400 | 0.3673 |  |  |  |
| SrO                            | 0.0154               | 0.0003 | 0.0000 | 0.0166 | 0.0000 | 0.0200 | 0.0200 | 0.0000 | 0.0000 |  |  |  |
| ThO <sub>2</sub>               | 0.0000               | 0.0000 | 0.0000 | 0.0000 | 0.0073 | 0.0114 | 0.0200 | 0.0200 | 0.0191 |  |  |  |
| TiO <sub>2</sub>               | 0.0154               | 0.0003 | 0.0060 | 0.0001 | 0.0000 | 0.0000 | 0.0173 | 0.0000 | 0.0078 |  |  |  |
| U <sub>3</sub> O <sub>8</sub>  | 0.0000               | 0.0000 | 0.0000 | 0.0000 | 0.0200 | 0.0261 | 0.0800 | 0.0200 | 0.0200 |  |  |  |
| ZnO                            | 0.0077               | 0.0004 | 0.0000 | 0.0005 | 0.0000 | 0.0000 | 0.0200 | 0.0000 | 0.0167 |  |  |  |
| ZrO <sub>2</sub>               | 0.0306               | 0.0185 | 0.0000 | 0.0186 | 0.0100 | 0.0100 | 0.0287 | 0.0300 | 0.0100 |  |  |  |
| Others                         | 0.0150               | 0.0222 | 0.0059 | 0.0082 | 0.0150 | 0.0150 | 0.0150 | 0.0150 | 0.0150 |  |  |  |

(a) SPA-1 to SPA-8 are outer-layer glasses, SPA-9 to SPA-35 are inner-layer glasses, SPA-36 is a center point, SPA-37 to SPA-40 are replicates (see text discussion), and SPA-41 to SPA-45 are radioactive glasses.

## Step 8: Assess the Combined Existing Glasses and New Experimental Design Glasses

Figure C.1 in Appendix C shows comparative dot plots of the normalized 21-components for the 144 existing glasses and the 45 new experimental design glasses. Scatterplot matrices also were used to view two-dimensional projections of the compositions and predicted spinel  $T_L$ , but are not presented here. The dot plots in Figure C.1 show reasonably good coverage of glass component ranges by existing and new glass compositions. New glasses partially filled in component ranges not covered or inadequately covered by existing glasses. However, because only 8 of 45 new glasses were on the outer layer of the experimental region, there were still a limited number of glasses with higher values of some components. Still, the dot plots suggested that the combined  $144 + 45 = 189$  glass data set would provide good support for fitting models relating spinel  $T_L$  to glass composition.

## 4.0 Summary

This paper discusses the application of non-traditional methods to construct a constrained mixture experiment design for studying the dependence of spinel  $T_L$  on nuclear waste glass composition. Because many components of waste glasses can impact spinel  $T_L$ , 19 nonradioactive components and 2 radioactive components were chosen to be varied in the design. Single- and multi-component constraints were specified to restrict attention to glass compositions appropriate for the nuclear wastes considered and having glass properties within desired ranges. A layered design approach was used to augment 144 existing glasses falling within a slightly expanded version of the glass composition experimental region. The layered design approach allowed selecting fewer new nonradioactive glasses (8) on the boundary (outer layer) of the experimental region, and more nonradioactive glasses (27) on an inner layer of the experimental region of more interest. The construction of a layered design in steps also allowed adding a center glass composition, replicates, and a small number (5) of radioactive glasses.

The large number of mixture components and component constraints made it impossible to use the traditional design construction approach of generating candidate points and selecting a subset using optimal experimental design. A coordinate-exchange algorithm modified for applicability to mixture experiments implemented in JMP (2000) was used. This algorithm generates optimal experimental designs without the need to first generate candidate points. This algorithm in JMP was used in sequential steps to augment existing glasses with the outer layer nonradioactive, inner layer nonradioactive, and radioactive glasses.

## 5.0 References

- AMERICAN SOCIETY FOR TESTING AND MATERIALS (ASTM). (1998). "Standard Test Methods for Determining Chemical Durability of Nuclear Waste Glasses: Product Consistency Test (PCT)". ASTM-C-1285-97, *1998 Annual Book of ASTM Standards*, West Conshohocken, PA.
- JIRICKA, M.; HRMA, P.; and VIENNA, J. D. (2001). "The Effect of Composition on Spinel Crystals Equilibrium in Low Silica High-Level Waste Glasses". Submitted to *Journal of Non-Crystalline Solids*.
- JMP. (2000). *JMP Version 4*. SAS Institute Inc., Cary, NC.
- KIRKBRIDE, R. A. (2000). *Tank Farm Contractor Operation and Utilization Plan (TWRS-OUP)*, HNF-SD-WM-SP-012, Rev. 2. CH2M Hill Hanford Group, Inc., Richland, WA.
- MEYER, R. K. and NACHTSHEIM, C. J. (1995). "The Coordinate Exchange Algorithm for Constructing Exact Optimal Designs". *Technometrics* 37, pp. 60-69.
- PIEPEL, G. F. (1982). "Measuring Component Effects in Constrained Mixture Experiments". *Technometrics* 24, pp. 29-39.
- PIEPEL, G. F. (1990). "Screening Designs for Constrained Mixture Experiments Derived from Classical Screening Designs". *Journal of Quality Technology* 22, pp. 23-33.
- PIEPEL, G. F. (1991). "Screening Designs for Constrained Mixture Experiments Derived from Classical Screening Designs—An Addendum". *Journal of Quality Technology* 23, pp. 96-101.
- PIEPEL, G. F. (1999). *MIXSOFT™ Software for the Design and Analysis of Mixture and Other Constrained Region Experiments, User's Guide, Version 2.31*, MIXSOFT--Mixture Experiment Software, Richland, WA.
- PIEPEL, G. F.; ANDERSON, C. M.; and REDGATE, P. E. (1993). "Response Surface Designs for Irregularly-Shaped Regions" (Parts 1, 2, and 3). *1993 Proceedings of the Section on Physical and Engineering Sciences*, pp. 205-227, American Statistical Association, Alexandria, VA.
- PIEPEL, G. F.; COOLEY, S. K.; PEELER, D. K.; VIENNA, J. D.; and EDWARDS, T. B. (2002). "Augmenting a Waste Glass Mixture Experiment Study with Additional Glass Components and Experimental Runs". *Quality Engineering* 15, pp. 91-111.
- VIENNA, J. D.; HRMA, P.; CRUM, J. V.; and MIKA, M. (2001). "Liquidus Temperature-Composition Model for Multi-Component Glasses in the Fe, Cr, Ni, and Mn Spinel Primary Phase Field". *Journal of Non-Crystalline Solids* 292, pp. 1-24.

## Appendix A

### A Candidate Set Free Approach to D-Optimal Mixture Design

Version 4.0 and later releases of JMP® are capable of generating optimal designs with or without candidate points. To generate optimal designs without candidate points, JMP uses a modification of the coordinate-exchange algorithm introduced by Meyer and Nachtsheim (1995). Row-exchange algorithms have traditionally been used to generate optimal designs from a set of candidate points.

Row-exchange algorithms replace an entire design row with a candidate set row at each step. The two important data structures are the current design and the candidate set. The objective function for the current design is compared to the objective function for a possible new design obtained by replacing a row of the current design by a row of the candidate set. Row exchanges are performed until the objective function is optimized. For the commonly used D-optimal design criterion, the goal is to minimize the objective function  $| (X'X)^{-1} |$ . Depending on the purpose of an experiment, the candidate set may include: 1) vertices, 2) other boundary points, and 3) interior points of the experimental region. For an unconstrained mixture experiment, the candidate points must be on or within the mixture simplex. For a constrained mixture experiment, the candidate points must be on or within the specified constrained subregion. As the number of mixture components and constraints defining a constrained mixture experiment increase, the number of candidate points grows rapidly. This means computing resources to generate and store the candidate points also grow rapidly with the numbers of mixture components and constraints.

By contrast, the coordinate-exchange algorithm replaces only one coordinate of a design row at each step. In a mixture experiment, each mixture component varies from a lower bound ( $0 \leq L_i$ ) to an upper bound ( $U_i \leq 1$ ). These lower and upper limit values, as well as an arbitrary number of points between them, are candidates for exchange of the current value.

However, there are two difficulties in applying a coordinate-exchange algorithm to mixture experiment design. First, a starting design of feasible mixture points must be generated to begin the coordinate-exchange algorithm. A mixture point is feasible if it lies on or within all the constraint boundaries and satisfies the mixture constraint (of the proportions summing to 1). Second, a coordinate value (mixture component proportion) cannot be changed independently of the other coordinates in a mixture. If a coordinate changes, then at least one other coordinate also must change to maintain the sum of the mixture component proportions at 1. The following discussion describes ways to overcome these two difficulties.

#### Step 1: Find a Starting Design of Feasible Points

One way to find a starting design is by generating feasible points one at a time until a starting design with the desired number of runs is obtained. The process starts by generating a random point within the mixture simplex. If this point obeys all the constraints, then it is added to the starting design. Otherwise, it is projected onto the nearest constraint boundary. If all constraints are satisfied, the point is added to the starting design. If not, the process continues by finding the nearest constraint boundary and projecting the point onto that boundary. If the constraint set is consistent, this process yields a feasible point. The process is repeated until a starting design with the desired number of feasible points is obtained.

## Step 2: Apply Coordinate-Exchange Algorithm to Optimize the Starting Design

After a starting design is constructed, a sequence of coordinate exchanges is performed to generate an optimal design. Starting with the first point of the starting design, the first component can be varied along with the remaining components so that the pair-wise ratios of the remaining components remain fixed. This yields a line that traces through the first point of the starting design to the vertex of the mixture simplex corresponding to the first component. This line is referred to as the Cox-effect direction (Piepel 1982, Cornell 2002) for the first component, where the first starting design point is the reference mixture. Performing coordinate exchanges in this manner overcomes the difficulty mentioned previously, that the proportion of one component cannot be changed independently.

If there are lower and upper bound constraints and/or linear inequality constraints on the mixture component proportions, the upper limit ( $U_1$ ) of the first mixture component may be less than one. Similarly, the lower limit ( $L_1$ ) may be greater than zero. Consider  $n - 1$  additional points obtained by dividing the segment of the Cox-effect direction of the first component between  $L_1$  and  $U_1$  into  $n$  sub-segments of equal length. For each of these  $n + 1$  points, the value of the objective function is computed. If the maximum improvement in the objective function is greater than zero, the current point is exchanged for the point corresponding to this increase.

Next, the second mixture component of the first point is used to repeat the process. The process continues until all components in all rows have been considered for exchange. If any exchanges were made, then the entire process is repeated starting with the first component in the first row. The coordinate-exchange algorithm ends when there have been no exchanges in a complete pass through all the components in every row. An alternative stopping rule is to put an upper bound on the number of iterations through the factor settings matrix.

## Other Considerations

It is desirable to repeat the entire coordinate-exchange algorithm (both Steps 1 and 2) using many random starting designs. While this does not guarantee convergence to a global optimum, it improves the chance of avoiding a poor but locally optimal design.

## **Appendix B**

### **Existing Glass Compositions Augmented by New Design**

Table B.1 contains the un-normalized 22-component mass-fraction compositions of the 144 screened, existing glass compositions in the spinel primary phase field chosen to be augmented with additional glasses. The mass fractions are rounded to four decimal places. Normalized 19-component and 21-component versions of these compositions were calculated according to Equations (5) and (6) in the main body of the paper.



Table B.1. Un-normalized 22-Component Mass-Fraction Compositions of the 144 Existing Database Glasses in the Spinel Primary Phase Field Chosen for Augmentation

| Component                      | Glass  |        |        |        |        |        |        |        |        |        |        |        |
|--------------------------------|--------|--------|--------|--------|--------|--------|--------|--------|--------|--------|--------|--------|
|                                | MS-1a  | MS-1b  | MS-2a  | MS-2b  | MS-3a  | MS-3b  | MS-4a  | MS-4b  | MS-5   | MS-6   | MS-7a  | MS-7b  |
| Al <sub>2</sub> O <sub>3</sub> | 0.0800 | 0.0800 | 0.0800 | 0.0800 | 0.0800 | 0.0800 | 0.0800 | 0.0800 | 0.0800 | 0.0800 | 0.0800 | 0.0800 |
| B <sub>2</sub> O <sub>3</sub>  | 0.0700 | 0.0700 | 0.0700 | 0.0700 | 0.0700 | 0.0700 | 0.0700 | 0.0700 | 0.0700 | 0.0700 | 0.0700 | 0.0700 |
| Bi <sub>2</sub> O <sub>3</sub> | 0.0000 | 0.0000 | 0.0000 | 0.0000 | 0.0000 | 0.0000 | 0.0000 | 0.0000 | 0.0000 | 0.0000 | 0.0000 | 0.0000 |
| CaO                            | 0.0000 | 0.0000 | 0.0000 | 0.0000 | 0.0000 | 0.0000 | 0.0000 | 0.0000 | 0.0000 | 0.0000 | 0.0000 | 0.0000 |
| CdO                            | 0.0000 | 0.0000 | 0.0000 | 0.0000 | 0.0000 | 0.0000 | 0.0000 | 0.0000 | 0.0000 | 0.0000 | 0.0000 | 0.0000 |
| Cr <sub>2</sub> O <sub>3</sub> | 0.0070 | 0.0070 | 0.0050 | 0.0050 | 0.0050 | 0.0050 | 0.0050 | 0.0050 | 0.0050 | 0.0035 | 0.0030 | 0.0030 |
| F                              | 0.0000 | 0.0000 | 0.0000 | 0.0000 | 0.0000 | 0.0000 | 0.0000 | 0.0000 | 0.0000 | 0.0000 | 0.0000 | 0.0000 |
| Fe <sub>2</sub> O <sub>3</sub> | 0.1300 | 0.1300 | 0.1450 | 0.1450 | 0.1150 | 0.1150 | 0.0889 | 0.0889 | 0.1150 | 0.1250 | 0.1150 | 0.1150 |
| K <sub>2</sub> O               | 0.0000 | 0.0000 | 0.0000 | 0.0000 | 0.0000 | 0.0000 | 0.0000 | 0.0000 | 0.0000 | 0.0000 | 0.0000 | 0.0000 |
| Li <sub>2</sub> O              | 0.0450 | 0.0450 | 0.0400 | 0.0400 | 0.0400 | 0.0400 | 0.0454 | 0.0454 | 0.0410 | 0.0300 | 0.0454 | 0.0454 |
| MnO                            | 0.0050 | 0.0050 | 0.0050 | 0.0050 | 0.0050 | 0.0050 | 0.0050 | 0.0050 | 0.0050 | 0.0036 | 0.0050 | 0.0050 |
| Na <sub>2</sub> O              | 0.1570 | 0.1570 | 0.1530 | 0.1530 | 0.1530 | 0.1530 | 0.1530 | 0.1530 | 0.1530 | 0.1573 | 0.1530 | 0.1530 |
| NiO                            | 0.0200 | 0.0200 | 0.0120 | 0.0120 | 0.0120 | 0.0120 | 0.0120 | 0.0120 | 0.0074 | 0.0140 | 0.0095 | 0.0095 |
| P <sub>2</sub> O <sub>5</sub>  | 0.0000 | 0.0000 | 0.0000 | 0.0000 | 0.0000 | 0.0000 | 0.0000 | 0.0000 | 0.0000 | 0.0000 | 0.0000 | 0.0000 |
| SiO <sub>2</sub>               | 0.4500 | 0.4500 | 0.4240 | 0.4240 | 0.4540 | 0.4540 | 0.4746 | 0.4746 | 0.4576 | 0.4600 | 0.4531 | 0.4531 |
| SrO                            | 0.0000 | 0.0000 | 0.0000 | 0.0000 | 0.0000 | 0.0000 | 0.0000 | 0.0000 | 0.0000 | 0.0000 | 0.0000 | 0.0000 |
| ThO <sub>2</sub>               | 0.0000 | 0.0000 | 0.0000 | 0.0000 | 0.0000 | 0.0000 | 0.0000 | 0.0000 | 0.0000 | 0.0000 | 0.0000 | 0.0000 |
| TiO <sub>2</sub>               | 0.0000 | 0.0000 | 0.0000 | 0.0000 | 0.0000 | 0.0000 | 0.0000 | 0.0000 | 0.0000 | 0.0000 | 0.0000 | 0.0000 |
| U <sub>3</sub> O <sub>8</sub>  | 0.0000 | 0.0000 | 0.0000 | 0.0000 | 0.0000 | 0.0000 | 0.0000 | 0.0000 | 0.0000 | 0.0000 | 0.0000 | 0.0000 |
| ZnO                            | 0.0000 | 0.0000 | 0.0000 | 0.0000 | 0.0000 | 0.0000 | 0.0000 | 0.0000 | 0.0000 | 0.0000 | 0.0000 | 0.0000 |
| ZrO <sub>2</sub>               | 0.0300 | 0.0300 | 0.0600 | 0.0600 | 0.0600 | 0.0600 | 0.0600 | 0.0600 | 0.0600 | 0.0506 | 0.0600 | 0.0600 |
| Others                         | 0.0060 | 0.0060 | 0.0060 | 0.0060 | 0.0060 | 0.0060 | 0.0060 | 0.0060 | 0.0060 | 0.0060 | 0.0060 | 0.0060 |

| Component                      | Glass  |        |        |          |          |          |          |          |          |          |          |          |
|--------------------------------|--------|--------|--------|----------|----------|----------|----------|----------|----------|----------|----------|----------|
|                                | MS-7c  | MS-7d  | MS-7e  | MS7-H-Al | MS7-L-Al | MS7-H-Cr | MS7-L-Cr | MS7-H-Fe | MS7-L-Fe | MS7-H-Li | MS7-L-Li | MS7-H-Mg |
| Al <sub>2</sub> O <sub>3</sub> | 0.0800 | 0.0800 | 0.0800 | 0.1100   | 0.0500   | 0.0789   | 0.0802   | 0.0768   | 0.0832   | 0.0788   | 0.0813   | 0.0781   |
| B <sub>2</sub> O <sub>3</sub>  | 0.0700 | 0.0700 | 0.0700 | 0.0677   | 0.0723   | 0.0699   | 0.0701   | 0.0672   | 0.0728   | 0.0689   | 0.0711   | 0.0683   |
| Bi <sub>2</sub> O <sub>3</sub> | 0.0000 | 0.0000 | 0.0000 | 0.0000   | 0.0000   | 0.0000   | 0.0000   | 0.0000   | 0.0000   | 0.0000   | 0.0000   | 0.0000   |
| CaO                            | 0.0000 | 0.0000 | 0.0000 | 0.0000   | 0.0000   | 0.0000   | 0.0000   | 0.0000   | 0.0000   | 0.0000   | 0.0000   | 0.0000   |
| CdO                            | 0.0000 | 0.0000 | 0.0000 | 0.0000   | 0.0000   | 0.0000   | 0.0000   | 0.0000   | 0.0000   | 0.0000   | 0.0000   | 0.0000   |
| Cr <sub>2</sub> O <sub>3</sub> | 0.0030 | 0.0030 | 0.0030 | 0.0029   | 0.0031   | 0.0050   | 0.0010   | 0.0029   | 0.0031   | 0.0030   | 0.0030   | 0.0029   |
| F                              | 0.0000 | 0.0000 | 0.0000 | 0.0000   | 0.0000   | 0.0000   | 0.0000   | 0.0000   | 0.0000   | 0.0000   | 0.0000   | 0.0000   |
| Fe <sub>2</sub> O <sub>3</sub> | 0.1150 | 0.1150 | 0.1150 | 0.1113   | 0.1180   | 0.1148   | 0.1152   | 0.1500   | 0.0800   | 0.1132   | 0.1169   | 0.1122   |
| K <sub>2</sub> O               | 0.0000 | 0.0000 | 0.0000 | 0.0000   | 0.0000   | 0.0000   | 0.0000   | 0.0000   | 0.0000   | 0.0000   | 0.0000   | 0.0000   |
| Li <sub>2</sub> O              | 0.0454 | 0.0454 | 0.0454 | 0.0439   | 0.0469   | 0.0453   | 0.0455   | 0.0436   | 0.0472   | 0.0600   | 0.0300   | 0.0443   |
| MnO                            | 0.0050 | 0.0050 | 0.0050 | 0.0048   | 0.0052   | 0.0050   | 0.0050   | 0.0048   | 0.0052   | 0.0049   | 0.0051   | 0.0049   |
| Na <sub>2</sub> O              | 0.1530 | 0.1530 | 0.1530 | 0.1480   | 0.1580   | 0.1527   | 0.1533   | 0.1469   | 0.1591   | 0.1507   | 0.1555   | 0.1493   |
| NiO                            | 0.0095 | 0.0095 | 0.0095 | 0.0092   | 0.0098   | 0.0095   | 0.0095   | 0.0091   | 0.0099   | 0.0094   | 0.0097   | 0.0093   |
| P <sub>2</sub> O <sub>5</sub>  | 0.0000 | 0.0000 | 0.0000 | 0.0000   | 0.0000   | 0.0000   | 0.0000   | 0.0000   | 0.0000   | 0.0000   | 0.0000   | 0.0000   |
| SiO <sub>2</sub>               | 0.4531 | 0.4531 | 0.4531 | 0.4383   | 0.4679   | 0.4522   | 0.4540   | 0.4352   | 0.4710   | 0.4462   | 0.4604   | 0.4422   |
| SrO                            | 0.0000 | 0.0000 | 0.0000 | 0.0000   | 0.0000   | 0.0000   | 0.0000   | 0.0000   | 0.0000   | 0.0000   | 0.0000   | 0.0000   |
| ThO <sub>2</sub>               | 0.0000 | 0.0000 | 0.0000 | 0.0000   | 0.0000   | 0.0000   | 0.0000   | 0.0000   | 0.0000   | 0.0000   | 0.0000   | 0.0000   |
| TiO <sub>2</sub>               | 0.0000 | 0.0000 | 0.0000 | 0.0000   | 0.0000   | 0.0000   | 0.0000   | 0.0000   | 0.0000   | 0.0000   | 0.0000   | 0.0000   |
| U <sub>3</sub> O <sub>8</sub>  | 0.0000 | 0.0000 | 0.0000 | 0.0000   | 0.0000   | 0.0000   | 0.0000   | 0.0000   | 0.0000   | 0.0000   | 0.0000   | 0.0000   |
| ZnO                            | 0.0000 | 0.0000 | 0.0000 | 0.0000   | 0.0000   | 0.0000   | 0.0000   | 0.0000   | 0.0000   | 0.0000   | 0.0000   | 0.0000   |
| ZrO <sub>2</sub>               | 0.0600 | 0.0600 | 0.0600 | 0.0580   | 0.0620   | 0.0599   | 0.0601   | 0.0576   | 0.0624   | 0.0591   | 0.0610   | 0.0586   |
| Others                         | 0.0060 | 0.0060 | 0.0060 | 0.0059   | 0.0068   | 0.0068   | 0.0061   | 0.0058   | 0.0062   | 0.0058   | 0.0060   | 0.0300   |

Table B.1. Un-normalized 22-Component Mass-Fraction Compositions of the 144 Existing Database Glasses in the Spinel Primary Phase Field Chosen for Augmentation (cont.)

| Component                      | Glass    |          |          |          |          |        |        |        |        |        |        |         |
|--------------------------------|----------|----------|----------|----------|----------|--------|--------|--------|--------|--------|--------|---------|
|                                | MS7-L-Mg | MS7-H-Na | MS7-L-Na | MS7-H-Ni | MS7-L-Ni | MS-8   | MS-9   | nom-2  | nom-3  | nomc-1 | nomc-2 | c106a-3 |
| Al <sub>2</sub> O <sub>3</sub> | 0.0805   | 0.0774   | 0.0831   | 0.0793   | 0.0805   | 0.0800 | 0.0800 | 0.0681 | 0.0808 | 0.0493 | 0.0412 | 0.1214  |
| B <sub>2</sub> O <sub>3</sub>  | 0.0704   | 0.0678   | 0.0727   | 0.0694   | 0.0705   | 0.0700 | 0.0700 | 0.0982 | 0.1093 | 0.0500 | 0.0588 | 0.0500  |
| Bi <sub>2</sub> O <sub>3</sub> | 0.0000   | 0.0000   | 0.0000   | 0.0000   | 0.0000   | 0.0000 | 0.0000 | 0.0000 | 0.0000 | 0.0000 | 0.0000 | 0.0000  |
| CaO                            | 0.0000   | 0.0000   | 0.0000   | 0.0000   | 0.0000   | 0.0000 | 0.0000 | 0.0086 | 0.0102 | 0.0119 | 0.0100 | 0.0261  |
| CdO                            | 0.0000   | 0.0000   | 0.0000   | 0.0000   | 0.0000   | 0.0000 | 0.0000 | 0.0057 | 0.0068 | 0.0080 | 0.0067 | 0.0006  |
| Cr <sub>2</sub> O <sub>3</sub> | 0.0030   | 0.0029   | 0.0031   | 0.0030   | 0.0030   | 0.0035 | 0.0100 | 0.0018 | 0.0022 | 0.0023 | 0.0019 | 0.0023  |
| F                              | 0.0000   | 0.0000   | 0.0000   | 0.0000   | 0.0000   | 0.0000 | 0.0000 | 0.0005 | 0.0006 | 0.0007 | 0.0005 | 0.0000  |
| Fe <sub>2</sub> O <sub>3</sub> | 0.1157   | 0.1113   | 0.1195   | 0.1140   | 0.1158   | 0.1250 | 0.1100 | 0.1076 | 0.1278 | 0.1500 | 0.1254 | 0.1170  |
| K <sub>2</sub> O               | 0.0000   | 0.0000   | 0.0000   | 0.0000   | 0.0000   | 0.0000 | 0.0000 | 0.0024 | 0.0029 | 0.0034 | 0.0028 | 0.0025  |
| Li <sub>2</sub> O              | 0.0457   | 0.0440   | 0.0472   | 0.0450   | 0.0457   | 0.0300 | 0.0400 | 0.0600 | 0.0100 | 0.0100 | 0.0521 | 0.0252  |
| MnO                            | 0.0050   | 0.0048   | 0.0052   | 0.0050   | 0.0050   | 0.0036 | 0.0036 | 0.0028 | 0.0033 | 0.0039 | 0.0033 | 0.0037  |
| Na <sub>2</sub> O              | 0.1539   | 0.1800   | 0.1200   | 0.1517   | 0.1540   | 0.1573 | 0.1573 | 0.0913 | 0.1733 | 0.1883 | 0.1177 | 0.1886  |
| NiO                            | 0.0096   | 0.0092   | 0.0099   | 0.0180   | 0.0030   | 0.0075 | 0.0100 | 0.0045 | 0.0053 | 0.0062 | 0.0052 | 0.0019  |
| P <sub>2</sub> O <sub>5</sub>  | 0.0000   | 0.0000   | 0.0000   | 0.0000   | 0.0000   | 0.0000 | 0.0000 | 0.0039 | 0.0046 | 0.0019 | 0.0015 | 0.0089  |
| SiO <sub>2</sub>               | 0.4558   | 0.4387   | 0.4708   | 0.4492   | 0.4561   | 0.4600 | 0.4531 | 0.5011 | 0.4113 | 0.4535 | 0.5221 | 0.4135  |
| SrO                            | 0.0000   | 0.0000   | 0.0000   | 0.0000   | 0.0000   | 0.0000 | 0.0000 | 0.0003 | 0.0003 | 0.0004 | 0.0003 | 0.0002  |
| ThO <sub>2</sub>               | 0.0000   | 0.0000   | 0.0000   | 0.0000   | 0.0000   | 0.0000 | 0.0000 | 0.0000 | 0.0000 | 0.0000 | 0.0000 | 0.0000  |
| TiO <sub>2</sub>               | 0.0000   | 0.0000   | 0.0000   | 0.0000   | 0.0000   | 0.0000 | 0.0000 | 0.0002 | 0.0003 | 0.0003 | 0.0003 | 0.0000  |
| U <sub>3</sub> O <sub>8</sub>  | 0.0000   | 0.0000   | 0.0000   | 0.0000   | 0.0000   | 0.0000 | 0.0000 | 0.0000 | 0.0000 | 0.0000 | 0.0000 | 0.0000  |
| ZnO                            | 0.0000   | 0.0000   | 0.0000   | 0.0000   | 0.0000   | 0.0000 | 0.0000 | 0.0002 | 0.0002 | 0.0002 | 0.0002 | 0.0001  |
| ZrO <sub>2</sub>               | 0.0604   | 0.0581   | 0.0623   | 0.0595   | 0.0604   | 0.0571 | 0.0600 | 0.0155 | 0.0184 | 0.0216 | 0.0181 | 0.0044  |
| Others                         | 0.0000   | 0.0058   | 0.0062   | 0.0059   | 0.0060   | 0.0060 | 0.0060 | 0.0273 | 0.0324 | 0.0381 | 0.0319 | 0.0336  |

| Component                      | Glass   |         |         |        |        |        |        |        |        |        |        |        |
|--------------------------------|---------|---------|---------|--------|--------|--------|--------|--------|--------|--------|--------|--------|
|                                | c106a-4 | c106b-1 | c106b-2 | az-3   | az-5   | SG03   | SG06a  | SG06b  | SG06c  | SG14   | SG16   | SG17   |
| Al <sub>2</sub> O <sub>3</sub> | 0.0940  | 0.1604  | 0.1440  | 0.0664 | 0.0554 | 0.0390 | 0.0799 | 0.0799 | 0.0800 | 0.0250 | 0.0664 | 0.0390 |
| B <sub>2</sub> O <sub>3</sub>  | 0.0831  | 0.1853  | 0.1094  | 0.0500 | 0.0974 | 0.0876 | 0.0500 | 0.0500 | 0.0500 | 0.0999 | 0.0626 | 0.0725 |
| Bi <sub>2</sub> O <sub>3</sub> | 0.0000  | 0.0000  | 0.0000  | 0.0000 | 0.0000 | 0.0000 | 0.0000 | 0.0000 | 0.0000 | 0.0000 | 0.0000 | 0.0000 |
| CaO                            | 0.0202  | 0.0020  | 0.0018  | 0.0031 | 0.0026 | 0.0158 | 0.0200 | 0.0200 | 0.0200 | 0.0030 | 0.0158 | 0.0158 |
| CdO                            | 0.0005  | 0.0000  | 0.0000  | 0.0102 | 0.0085 | 0.0000 | 0.0000 | 0.0000 | 0.0000 | 0.0000 | 0.0000 | 0.0000 |
| Cr <sub>2</sub> O <sub>3</sub> | 0.0017  | 0.0019  | 0.0017  | 0.0022 | 0.0018 | 0.0025 | 0.0010 | 0.0010 | 0.0010 | 0.0010 | 0.0015 | 0.0015 |
| F                              | 0.0000  | 0.0000  | 0.0000  | 0.0007 | 0.0006 | 0.0000 | 0.0000 | 0.0000 | 0.0000 | 0.0000 | 0.0000 | 0.0000 |
| Fe <sub>2</sub> O <sub>3</sub> | 0.0906  | 0.0871  | 0.0781  | 0.1397 | 0.1164 | 0.1202 | 0.1499 | 0.1499 | 0.1500 | 0.1499 | 0.0825 | 0.1275 |
| K <sub>2</sub> O               | 0.0019  | 0.0000  | 0.0000  | 0.0032 | 0.0027 | 0.0208 | 0.0380 | 0.0380 | 0.0380 | 0.0380 | 0.0208 | 0.0323 |
| Li <sub>2</sub> O              | 0.0402  | 0.0351  | 0.0599  | 0.0100 | 0.0149 | 0.0375 | 0.0300 | 0.0300 | 0.0300 | 0.0300 | 0.0525 | 0.0525 |
| MnO                            | 0.0029  | 0.0043  | 0.0039  | 0.0031 | 0.0026 | 0.0250 | 0.0100 | 0.0100 | 0.0100 | 0.0300 | 0.0250 | 0.0150 |
| Na <sub>2</sub> O              | 0.1461  | 0.1316  | 0.1311  | 0.2114 | 0.1796 | 0.0976 | 0.1099 | 0.1099 | 0.1100 | 0.1099 | 0.0976 | 0.0976 |
| NiO                            | 0.0015  | 0.0000  | 0.0000  | 0.0079 | 0.0060 | 0.0151 | 0.0005 | 0.0005 | 0.0005 | 0.0005 | 0.0054 | 0.0151 |
| P <sub>2</sub> O <sub>5</sub>  | 0.0069  | 0.0105  | 0.0094  | 0.0027 | 0.0023 | 0.0000 | 0.0000 | 0.0000 | 0.0000 | 0.0000 | 0.0000 | 0.0000 |
| SiO <sub>2</sub>               | 0.4806  | 0.3700  | 0.4501  | 0.4296 | 0.4588 | 0.4741 | 0.4991 | 0.4991 | 0.4994 | 0.4306 | 0.5026 | 0.4741 |
| SrO                            | 0.0001  | 0.0001  | 0.0001  | 0.0004 | 0.0003 | 0.0000 | 0.0000 | 0.0000 | 0.0000 | 0.0000 | 0.0000 | 0.0000 |
| ThO <sub>2</sub>               | 0.0000  | 0.0000  | 0.0000  | 0.0000 | 0.0000 | 0.0000 | 0.0000 | 0.0000 | 0.0000 | 0.0000 | 0.0000 | 0.0000 |
| TiO <sub>2</sub>               | 0.0000  | 0.0004  | 0.0004  | 0.0004 | 0.0004 | 0.0026 | 0.0060 | 0.0060 | 0.0060 | 0.0015 | 0.0049 | 0.0049 |
| U <sub>3</sub> O <sub>8</sub>  | 0.0000  | 0.0000  | 0.0000  | 0.0000 | 0.0000 | 0.0415 | 0.0000 | 0.0000 | 0.0000 | 0.0550 | 0.0415 | 0.0415 |
| ZnO                            | 0.0001  | 0.0001  | 0.0001  | 0.0003 | 0.0002 | 0.0000 | 0.0000 | 0.0000 | 0.0000 | 0.0000 | 0.0000 | 0.0000 |
| ZrO <sub>2</sub>               | 0.0034  | 0.0006  | 0.0005  | 0.0264 | 0.0220 | 0.0000 | 0.0000 | 0.0000 | 0.0000 | 0.0000 | 0.0000 | 0.0000 |
| Others                         | 0.0262  | 0.0106  | 0.0095  | 0.0323 | 0.0275 | 0.0209 | 0.0059 | 0.0059 | 0.0053 | 0.0259 | 0.0209 | 0.0109 |

Table B.1. Un-normalized 22-Component Mass-Fraction Compositions of the 144 Existing Database Glasses in the Spinel Primary Phase Field Chosen for Augmentation (cont.)

| Component                      | Glass  |        |        |        |        |        |        |        |        |        |        |        |
|--------------------------------|--------|--------|--------|--------|--------|--------|--------|--------|--------|--------|--------|--------|
|                                | SG18a  | SG18b  | SG18c  | SG18d  | SG18e  | SG18f  | SG18g  | SG19   | SG22   | SG26   | SG29   | SG30   |
| Al <sub>2</sub> O <sub>3</sub> | 0.0250 | 0.0250 | 0.0250 | 0.0250 | 0.0250 | 0.0250 | 0.0250 | 0.0799 | 0.0664 | 0.0390 | 0.0799 | 0.0799 |
| B <sub>2</sub> O <sub>3</sub>  | 0.0999 | 0.0999 | 0.0999 | 0.0999 | 0.0999 | 0.0999 | 0.0999 | 0.0999 | 0.0626 | 0.0626 | 0.0500 | 0.0500 |
| Bi <sub>2</sub> O <sub>3</sub> | 0.0000 | 0.0000 | 0.0000 | 0.0000 | 0.0000 | 0.0000 | 0.0000 | 0.0000 | 0.0000 | 0.0000 | 0.0000 | 0.0000 |
| CaO                            | 0.0030 | 0.0030 | 0.0030 | 0.0030 | 0.0030 | 0.0030 | 0.0030 | 0.0030 | 0.0158 | 0.0073 | 0.0030 | 0.0200 |
| CdO                            | 0.0000 | 0.0000 | 0.0000 | 0.0000 | 0.0000 | 0.0000 | 0.0000 | 0.0000 | 0.0000 | 0.0000 | 0.0000 | 0.0000 |
| Cr <sub>2</sub> O <sub>3</sub> | 0.0030 | 0.0030 | 0.0030 | 0.0030 | 0.0030 | 0.0030 | 0.0030 | 0.0030 | 0.0025 | 0.0025 | 0.0010 | 0.0010 |
| F                              | 0.0000 | 0.0000 | 0.0000 | 0.0000 | 0.0000 | 0.0000 | 0.0000 | 0.0000 | 0.0000 | 0.0000 | 0.0000 | 0.0000 |
| Fe <sub>2</sub> O <sub>3</sub> | 0.1499 | 0.1499 | 0.1499 | 0.1499 | 0.1499 | 0.1499 | 0.1499 | 0.0599 | 0.1275 | 0.1275 | 0.0599 | 0.0599 |
| K <sub>2</sub> O               | 0.0150 | 0.0150 | 0.0150 | 0.0150 | 0.0150 | 0.0150 | 0.0150 | 0.0380 | 0.0208 | 0.0208 | 0.0150 | 0.0380 |
| Li <sub>2</sub> O              | 0.0599 | 0.0599 | 0.0599 | 0.0599 | 0.0599 | 0.0599 | 0.0599 | 0.0599 | 0.0525 | 0.0375 | 0.0599 | 0.0599 |
| MnO                            | 0.0300 | 0.0300 | 0.0300 | 0.0300 | 0.0300 | 0.0300 | 0.0300 | 0.0100 | 0.0150 | 0.0150 | 0.0300 | 0.0300 |
| Na <sub>2</sub> O              | 0.1099 | 0.1099 | 0.1099 | 0.1099 | 0.1099 | 0.1099 | 0.1099 | 0.1099 | 0.0976 | 0.0976 | 0.1099 | 0.1099 |
| NiO                            | 0.0005 | 0.0005 | 0.0005 | 0.0005 | 0.0005 | 0.0005 | 0.0005 | 0.0200 | 0.0151 | 0.0054 | 0.0005 | 0.0200 |
| P <sub>2</sub> O <sub>5</sub>  | 0.0000 | 0.0000 | 0.0000 | 0.0000 | 0.0000 | 0.0000 | 0.0000 | 0.0000 | 0.0000 | 0.0000 | 0.0000 | 0.0000 |
| SiO <sub>2</sub>               | 0.4921 | 0.4921 | 0.4921 | 0.4921 | 0.4921 | 0.4921 | 0.4921 | 0.4541 | 0.4931 | 0.5276 | 0.5240 | 0.4491 |
| SrO                            | 0.0000 | 0.0000 | 0.0000 | 0.0000 | 0.0000 | 0.0000 | 0.0000 | 0.0000 | 0.0000 | 0.0000 | 0.0000 | 0.0000 |
| ThO <sub>2</sub>               | 0.0000 | 0.0000 | 0.0000 | 0.0000 | 0.0000 | 0.0000 | 0.0000 | 0.0000 | 0.0000 | 0.0000 | 0.0000 | 0.0000 |
| TiO <sub>2</sub>               | 0.0060 | 0.0060 | 0.0060 | 0.0060 | 0.0060 | 0.0060 | 0.0060 | 0.0015 | 0.0026 | 0.0049 | 0.0060 | 0.0015 |
| U <sub>3</sub> O <sub>8</sub>  | 0.0000 | 0.0000 | 0.0000 | 0.0000 | 0.0000 | 0.0000 | 0.0000 | 0.0550 | 0.0177 | 0.0415 | 0.0550 | 0.0550 |
| ZnO                            | 0.0000 | 0.0000 | 0.0000 | 0.0000 | 0.0000 | 0.0000 | 0.0000 | 0.0000 | 0.0000 | 0.0000 | 0.0000 | 0.0000 |
| ZrO <sub>2</sub>               | 0.0000 | 0.0000 | 0.0000 | 0.0000 | 0.0000 | 0.0000 | 0.0000 | 0.0000 | 0.0000 | 0.0000 | 0.0000 | 0.0000 |
| Others                         | 0.0059 | 0.0059 | 0.0059 | 0.0059 | 0.0059 | 0.0059 | 0.0059 | 0.0059 | 0.0109 | 0.0109 | 0.0059 | 0.0259 |

| Component                      | Glass  |        |        |        |        |        |        |        |        |        |        |        |
|--------------------------------|--------|--------|--------|--------|--------|--------|--------|--------|--------|--------|--------|--------|
|                                | SG32   | SG33   | SG35   | SG38   | SG39   | SG40   | SG42   | SG43   | SG47   | SG51   | SG52a  | SG52b  |
| Al <sub>2</sub> O <sub>3</sub> | 0.0799 | 0.0799 | 0.0799 | 0.0250 | 0.0250 | 0.0799 | 0.0449 | 0.0664 | 0.0250 | 0.0799 | 0.0250 | 0.0250 |
| B <sub>2</sub> O <sub>3</sub>  | 0.0999 | 0.0999 | 0.0500 | 0.0999 | 0.0500 | 0.0999 | 0.0876 | 0.0876 | 0.0500 | 0.0500 | 0.0999 | 0.0999 |
| Bi <sub>2</sub> O <sub>3</sub> | 0.0000 | 0.0000 | 0.0000 | 0.0000 | 0.0000 | 0.0000 | 0.0000 | 0.0000 | 0.0000 | 0.0000 | 0.0000 | 0.0000 |
| CaO                            | 0.0030 | 0.0200 | 0.0030 | 0.0030 | 0.0200 | 0.0030 | 0.0073 | 0.0073 | 0.0200 | 0.0200 | 0.0030 | 0.0030 |
| CdO                            | 0.0000 | 0.0000 | 0.0000 | 0.0000 | 0.0000 | 0.0000 | 0.0000 | 0.0000 | 0.0000 | 0.0000 | 0.0000 | 0.0000 |
| Cr <sub>2</sub> O <sub>3</sub> | 0.0010 | 0.0030 | 0.0030 | 0.0010 | 0.0030 | 0.0030 | 0.0025 | 0.0015 | 0.0030 | 0.0030 | 0.0030 | 0.0030 |
| F                              | 0.0000 | 0.0000 | 0.0000 | 0.0000 | 0.0000 | 0.0000 | 0.0000 | 0.0000 | 0.0000 | 0.0000 | 0.0000 | 0.0000 |
| Fe <sub>2</sub> O <sub>3</sub> | 0.1499 | 0.0599 | 0.1449 | 0.1464 | 0.1499 | 0.0599 | 0.1275 | 0.0825 | 0.1499 | 0.1499 | 0.1499 | 0.1499 |
| K <sub>2</sub> O               | 0.0150 | 0.0380 | 0.0380 | 0.0380 | 0.0150 | 0.0150 | 0.0323 | 0.0323 | 0.0150 | 0.0380 | 0.0150 | 0.0150 |
| Li <sub>2</sub> O              | 0.0599 | 0.0599 | 0.0599 | 0.0300 | 0.0300 | 0.0300 | 0.0525 | 0.0375 | 0.0599 | 0.0300 | 0.0599 | 0.0599 |
| MnO                            | 0.0100 | 0.0300 | 0.0300 | 0.0300 | 0.0300 | 0.0100 | 0.0250 | 0.0250 | 0.0100 | 0.0100 | 0.0300 | 0.0300 |
| Na <sub>2</sub> O              | 0.1099 | 0.1099 | 0.1099 | 0.1099 | 0.1099 | 0.1099 | 0.0976 | 0.0976 | 0.1099 | 0.1099 | 0.1099 | 0.1099 |
| NiO                            | 0.0200 | 0.0200 | 0.0200 | 0.0005 | 0.0200 | 0.0200 | 0.0054 | 0.0054 | 0.0200 | 0.0005 | 0.0005 | 0.0005 |
| P <sub>2</sub> O <sub>5</sub>  | 0.0000 | 0.0000 | 0.0000 | 0.0000 | 0.0000 | 0.0000 | 0.0000 | 0.0000 | 0.0000 | 0.0000 | 0.0000 | 0.0000 |
| SiO <sub>2</sub>               | 0.4396 | 0.4676 | 0.4296 | 0.4296 | 0.5355 | 0.4826 | 0.4741 | 0.5257 | 0.4551 | 0.5015 | 0.4921 | 0.4921 |
| SrO                            | 0.0000 | 0.0000 | 0.0000 | 0.0000 | 0.0000 | 0.0000 | 0.0000 | 0.0000 | 0.0000 | 0.0000 | 0.0000 | 0.0000 |
| ThO <sub>2</sub>               | 0.0000 | 0.0000 | 0.0000 | 0.0000 | 0.0000 | 0.0000 | 0.0000 | 0.0000 | 0.0000 | 0.0000 | 0.0000 | 0.0000 |
| TiO <sub>2</sub>               | 0.0060 | 0.0060 | 0.0060 | 0.0060 | 0.0060 | 0.0060 | 0.0049 | 0.0026 | 0.0015 | 0.0015 | 0.0060 | 0.0060 |
| U <sub>3</sub> O <sub>8</sub>  | 0.0000 | 0.0000 | 0.0000 | 0.0550 | 0.0000 | 0.0550 | 0.0177 | 0.0177 | 0.0550 | 0.0000 | 0.0000 | 0.0000 |
| ZnO                            | 0.0000 | 0.0000 | 0.0000 | 0.0000 | 0.0000 | 0.0000 | 0.0000 | 0.0000 | 0.0000 | 0.0000 | 0.0000 | 0.0000 |
| ZrO <sub>2</sub>               | 0.0000 | 0.0000 | 0.0000 | 0.0000 | 0.0000 | 0.0000 | 0.0000 | 0.0000 | 0.0000 | 0.0000 | 0.0000 | 0.0000 |
| Others                         | 0.0059 | 0.0059 | 0.0259 | 0.0259 | 0.0059 | 0.0259 | 0.0209 | 0.0109 | 0.0259 | 0.0059 | 0.0059 | 0.0059 |

Table B.1. Un-normalized 22-Component Mass-Fraction Compositions of the 144 Existing Database Glasses in the Spinel Primary Phase Field Chosen for Augmentation (cont.)

| Component                      | Glass  |        |        |        |        |        |        |        |        |        |        |        |
|--------------------------------|--------|--------|--------|--------|--------|--------|--------|--------|--------|--------|--------|--------|
|                                | SG52c  | SG52d  | SG52e  | SP-1a  | SP-1b  | SP-1c  | SP-1d  | SP-1e  | SP-1f  | SP-1g  | SP-1h  | SP-1i  |
| Al <sub>2</sub> O <sub>3</sub> | 0.0250 | 0.0250 | 0.0250 | 0.0800 | 0.0800 | 0.0800 | 0.0800 | 0.0800 | 0.0800 | 0.0800 | 0.0800 | 0.0800 |
| B <sub>2</sub> O <sub>3</sub>  | 0.0999 | 0.0999 | 0.0999 | 0.0700 | 0.0700 | 0.0700 | 0.0700 | 0.0700 | 0.0700 | 0.0700 | 0.0700 | 0.0700 |
| Bi <sub>2</sub> O <sub>3</sub> | 0.0000 | 0.0000 | 0.0000 | 0.0000 | 0.0000 | 0.0000 | 0.0000 | 0.0000 | 0.0000 | 0.0000 | 0.0000 | 0.0000 |
| CaO                            | 0.0030 | 0.0030 | 0.0030 | 0.0100 | 0.0100 | 0.0100 | 0.0100 | 0.0100 | 0.0100 | 0.0100 | 0.0100 | 0.0100 |
| CdO                            | 0.0000 | 0.0000 | 0.0000 | 0.0070 | 0.0070 | 0.0070 | 0.0070 | 0.0070 | 0.0070 | 0.0070 | 0.0070 | 0.0070 |
| Cr <sub>2</sub> O <sub>3</sub> | 0.0030 | 0.0030 | 0.0030 | 0.0022 | 0.0022 | 0.0022 | 0.0022 | 0.0022 | 0.0022 | 0.0022 | 0.0022 | 0.0022 |
| F                              | 0.0000 | 0.0000 | 0.0000 | 0.0006 | 0.0006 | 0.0006 | 0.0006 | 0.0006 | 0.0006 | 0.0006 | 0.0006 | 0.0006 |
| Fe <sub>2</sub> O <sub>3</sub> | 0.1499 | 0.1499 | 0.1499 | 0.1250 | 0.1250 | 0.1250 | 0.1250 | 0.1250 | 0.1250 | 0.1250 | 0.1250 | 0.1250 |
| K <sub>2</sub> O               | 0.0150 | 0.0150 | 0.0150 | 0.0028 | 0.0028 | 0.0028 | 0.0028 | 0.0028 | 0.0028 | 0.0028 | 0.0028 | 0.0028 |
| Li <sub>2</sub> O              | 0.0599 | 0.0599 | 0.0599 | 0.0300 | 0.0300 | 0.0300 | 0.0300 | 0.0300 | 0.0300 | 0.0300 | 0.0300 | 0.0300 |
| MnO                            | 0.0300 | 0.0300 | 0.0300 | 0.0036 | 0.0036 | 0.0036 | 0.0036 | 0.0036 | 0.0036 | 0.0036 | 0.0036 | 0.0036 |
| Na <sub>2</sub> O              | 0.1099 | 0.1099 | 0.1099 | 0.1573 | 0.1573 | 0.1573 | 0.1573 | 0.1573 | 0.1573 | 0.1573 | 0.1573 | 0.1573 |
| NiO                            | 0.0005 | 0.0005 | 0.0005 | 0.0052 | 0.0052 | 0.0052 | 0.0052 | 0.0052 | 0.0052 | 0.0052 | 0.0052 | 0.0052 |
| P <sub>2</sub> O <sub>5</sub>  | 0.0000 | 0.0000 | 0.0000 | 0.0046 | 0.0046 | 0.0046 | 0.0046 | 0.0046 | 0.0046 | 0.0046 | 0.0046 | 0.0046 |
| SiO <sub>2</sub>               | 0.4921 | 0.4921 | 0.4921 | 0.4600 | 0.4600 | 0.4600 | 0.4600 | 0.4600 | 0.4600 | 0.4600 | 0.4600 | 0.4600 |
| SrO                            | 0.0000 | 0.0000 | 0.0000 | 0.0003 | 0.0003 | 0.0003 | 0.0003 | 0.0003 | 0.0003 | 0.0003 | 0.0003 | 0.0003 |
| ThO <sub>2</sub>               | 0.0000 | 0.0000 | 0.0000 | 0.0000 | 0.0000 | 0.0000 | 0.0000 | 0.0000 | 0.0000 | 0.0000 | 0.0000 | 0.0000 |
| TiO <sub>2</sub>               | 0.0060 | 0.0060 | 0.0060 | 0.0003 | 0.0003 | 0.0003 | 0.0003 | 0.0003 | 0.0003 | 0.0003 | 0.0003 | 0.0003 |
| U <sub>3</sub> O <sub>8</sub>  | 0.0000 | 0.0000 | 0.0000 | 0.0000 | 0.0000 | 0.0000 | 0.0000 | 0.0000 | 0.0000 | 0.0000 | 0.0000 | 0.0000 |
| ZnO                            | 0.0000 | 0.0000 | 0.0000 | 0.0004 | 0.0004 | 0.0004 | 0.0004 | 0.0004 | 0.0004 | 0.0004 | 0.0004 | 0.0004 |
| ZrO <sub>2</sub>               | 0.0000 | 0.0000 | 0.0000 | 0.0185 | 0.0185 | 0.0185 | 0.0185 | 0.0185 | 0.0185 | 0.0185 | 0.0185 | 0.0185 |
| Others                         | 0.0059 | 0.0059 | 0.0059 | 0.0222 | 0.0222 | 0.0222 | 0.0222 | 0.0222 | 0.0222 | 0.0222 | 0.0222 | 0.0222 |

| Component                      | Glass   |         |        |        |        |         |         |         |         |         |         |         |
|--------------------------------|---------|---------|--------|--------|--------|---------|---------|---------|---------|---------|---------|---------|
|                                | SP-Al-1 | SP-Al-2 | SP-B-3 | SP-B-4 | SP-B-5 | SP-Ca-1 | SP-Cr-1 | SP-Cr-2 | SP-Cr-3 | SP-Cr-4 | SP-Fe-1 | SP-Fe-2 |
| Al <sub>2</sub> O <sub>3</sub> | 0.0400  | 0.1200  | 0.0826 | 0.0757 | 0.0688 | 0.0784  | 0.0802  | 0.0798  | 0.0795  | 0.0792  | 0.0859  | 0.0832  |
| B <sub>2</sub> O <sub>3</sub>  | 0.0730  | 0.0670  | 0.0400 | 0.1200 | 0.2000 | 0.0686  | 0.0702  | 0.0698  | 0.0696  | 0.0693  | 0.0752  | 0.0728  |
| Bi <sub>2</sub> O <sub>3</sub> | 0.0000  | 0.0000  | 0.0000 | 0.0000 | 0.0000 | 0.0000  | 0.0000  | 0.0000  | 0.0000  | 0.0000  | 0.0000  | 0.0000  |
| CaO                            | 0.0104  | 0.0096  | 0.0103 | 0.0095 | 0.0086 | 0.0300  | 0.0100  | 0.0100  | 0.0099  | 0.0099  | 0.0107  | 0.0104  |
| CdO                            | 0.0073  | 0.0067  | 0.0072 | 0.0066 | 0.0060 | 0.0068  | 0.0070  | 0.0069  | 0.0069  | 0.0069  | 0.0075  | 0.0072  |
| Cr <sub>2</sub> O <sub>3</sub> | 0.0023  | 0.0021  | 0.0023 | 0.0021 | 0.0019 | 0.0022  | 0.0000  | 0.0050  | 0.0080  | 0.0120  | 0.0024  | 0.0023  |
| F                              | 0.0006  | 0.0006  | 0.0006 | 0.0006 | 0.0005 | 0.0006  | 0.0006  | 0.0006  | 0.0006  | 0.0006  | 0.0007  | 0.0006  |
| Fe <sub>2</sub> O <sub>3</sub> | 0.1304  | 0.1196  | 0.1290 | 0.1183 | 0.1075 | 0.1225  | 0.1253  | 0.1246  | 0.1243  | 0.1238  | 0.0600  | 0.0900  |
| K <sub>2</sub> O               | 0.0029  | 0.0027  | 0.0029 | 0.0026 | 0.0024 | 0.0027  | 0.0028  | 0.0028  | 0.0028  | 0.0028  | 0.0030  | 0.0029  |
| Li <sub>2</sub> O              | 0.0313  | 0.0287  | 0.0310 | 0.0284 | 0.0258 | 0.0294  | 0.0301  | 0.0299  | 0.0298  | 0.0297  | 0.0322  | 0.0312  |
| MnO                            | 0.0038  | 0.0034  | 0.0037 | 0.0034 | 0.0031 | 0.0036  | 0.0036  | 0.0036  | 0.0036  | 0.0036  | 0.0039  | 0.0037  |
| Na <sub>2</sub> O              | 0.1641  | 0.1505  | 0.1624 | 0.1488 | 0.1353 | 0.1541  | 0.1576  | 0.1569  | 0.1564  | 0.1558  | 0.1690  | 0.1636  |
| NiO                            | 0.0054  | 0.0050  | 0.0054 | 0.0049 | 0.0045 | 0.0051  | 0.0052  | 0.0052  | 0.0052  | 0.0051  | 0.0056  | 0.0054  |
| P <sub>2</sub> O <sub>5</sub>  | 0.0048  | 0.0044  | 0.0048 | 0.0044 | 0.0040 | 0.0045  | 0.0047  | 0.0046  | 0.0046  | 0.0046  | 0.0050  | 0.0048  |
| SiO <sub>2</sub>               | 0.4800  | 0.4400  | 0.4748 | 0.4353 | 0.3957 | 0.4507  | 0.4610  | 0.4587  | 0.4573  | 0.4555  | 0.4942  | 0.4784  |
| SrO                            | 0.0003  | 0.0003  | 0.0003 | 0.0003 | 0.0003 | 0.0003  | 0.0003  | 0.0003  | 0.0003  | 0.0003  | 0.0003  | 0.0003  |
| ThO <sub>2</sub>               | 0.0000  | 0.0000  | 0.0000 | 0.0000 | 0.0000 | 0.0000  | 0.0000  | 0.0000  | 0.0000  | 0.0000  | 0.0000  | 0.0000  |
| TiO <sub>2</sub>               | 0.0003  | 0.0003  | 0.0003 | 0.0003 | 0.0003 | 0.0003  | 0.0003  | 0.0003  | 0.0003  | 0.0003  | 0.0003  | 0.0003  |
| U <sub>3</sub> O <sub>8</sub>  | 0.0000  | 0.0000  | 0.0000 | 0.0000 | 0.0000 | 0.0000  | 0.0000  | 0.0000  | 0.0000  | 0.0000  | 0.0000  | 0.0000  |
| ZnO                            | 0.0004  | 0.0004  | 0.0004 | 0.0004 | 0.0003 | 0.0004  | 0.0004  | 0.0004  | 0.0004  | 0.0004  | 0.0004  | 0.0004  |
| ZrO <sub>2</sub>               | 0.0193  | 0.0177  | 0.0191 | 0.0175 | 0.0159 | 0.0181  | 0.0185  | 0.0184  | 0.0184  | 0.0183  | 0.0198  | 0.0192  |
| Others                         | 0.0232  | 0.0212  | 0.0229 | 0.0210 | 0.0191 | 0.0217  | 0.0223  | 0.0222  | 0.0221  | 0.0220  | 0.0239  | 0.0231  |

Table B.1. Un-normalized 22-Component Mass-Fraction Compositions of the 144 Existing Database Glasses in the Spinel Primary Phase Field Chosen for Augmentation (cont.)

| Component                      | Glass   |        |        |         |         |         |         |         |         |         |         |         |
|--------------------------------|---------|--------|--------|---------|---------|---------|---------|---------|---------|---------|---------|---------|
|                                | SP-Fe-3 | SP-K-1 | SP-K-2 | SP-Li-3 | SP-Li-5 | SP-Mg-1 | SP-Mg-2 | SP-Mg-3 | SP-Mn-1 | SP-Mn-2 | SP-Mn-3 | SP-Na-2 |
| Al <sub>2</sub> O <sub>3</sub> | 0.0777  | 0.0786 | 0.0770 | 0.0800  | 0.0788  | 0.0797  | 0.0789  | 0.0757  | 0.0803  | 0.0795  | 0.0771  | 0.0835  |
| B <sub>2</sub> O <sub>3</sub>  | 0.0680  | 0.0688 | 0.0674 | 0.0700  | 0.0689  | 0.0697  | 0.0690  | 0.0662  | 0.0703  | 0.0696  | 0.0674  | 0.0731  |
| Bi <sub>2</sub> O <sub>3</sub> | 0.0000  | 0.0000 | 0.0000 | 0.0000  | 0.0000  | 0.0000  | 0.0000  | 0.0000  | 0.0000  | 0.0000  | 0.0000  | 0.0000  |
| CaO                            | 0.0097  | 0.0098 | 0.0096 | 0.0100  | 0.0098  | 0.0100  | 0.0099  | 0.0095  | 0.0100  | 0.0099  | 0.0096  | 0.0104  |
| CdO                            | 0.0068  | 0.0068 | 0.0067 | 0.0070  | 0.0068  | 0.0069  | 0.0069  | 0.0066  | 0.0070  | 0.0069  | 0.0067  | 0.0073  |
| Cr <sub>2</sub> O <sub>3</sub> | 0.0021  | 0.0022 | 0.0021 | 0.0022  | 0.0022  | 0.0022  | 0.0022  | 0.0021  | 0.0022  | 0.0022  | 0.0021  | 0.0023  |
| F                              | 0.0006  | 0.0006 | 0.0006 | 0.0006  | 0.0006  | 0.0006  | 0.0006  | 0.0006  | 0.0006  | 0.0006  | 0.0006  | 0.0006  |
| Fe <sub>2</sub> O <sub>3</sub> | 0.1500  | 0.1228 | 0.1203 | 0.1250  | 0.1231  | 0.1245  | 0.1232  | 0.1182  | 0.1255  | 0.1242  | 0.1204  | 0.1305  |
| K <sub>2</sub> O               | 0.0027  | 0.0200 | 0.0400 | 0.0028  | 0.0028  | 0.0028  | 0.0028  | 0.0026  | 0.0028  | 0.0028  | 0.0027  | 0.0029  |
| Li <sub>2</sub> O              | 0.0291  | 0.0295 | 0.0289 | 0.0300  | 0.0450  | 0.0299  | 0.0296  | 0.0284  | 0.0301  | 0.0298  | 0.0289  | 0.0313  |
| MnO                            | 0.0035  | 0.0036 | 0.0035 | 0.0036  | 0.0036  | 0.0036  | 0.0035  | 0.0034  | 0.0000  | 0.0100  | 0.0400  | 0.0038  |
| Na <sub>2</sub> O              | 0.1528  | 0.1546 | 0.1514 | 0.1573  | 0.1549  | 0.1567  | 0.1551  | 0.1488  | 0.1579  | 0.1563  | 0.1516  | 0.1200  |
| NiO                            | 0.0051  | 0.0051 | 0.0050 | 0.0052  | 0.0051  | 0.0052  | 0.0051  | 0.0049  | 0.0052  | 0.0052  | 0.0050  | 0.0054  |
| P <sub>2</sub> O <sub>5</sub>  | 0.0045  | 0.0045 | 0.0045 | 0.0046  | 0.0046  | 0.0046  | 0.0046  | 0.0044  | 0.0047  | 0.0046  | 0.0045  | 0.0049  |
| SiO <sub>2</sub>               | 0.4469  | 0.4521 | 0.4428 | 0.4600  | 0.4529  | 0.4581  | 0.4535  | 0.4350  | 0.4617  | 0.4570  | 0.4432  | 0.4804  |
| SrO                            | 0.0003  | 0.0003 | 0.0003 | 0.0003  | 0.0003  | 0.0003  | 0.0003  | 0.0003  | 0.0003  | 0.0003  | 0.0003  | 0.0003  |
| ThO <sub>2</sub>               | 0.0000  | 0.0000 | 0.0000 | 0.0000  | 0.0000  | 0.0000  | 0.0000  | 0.0000  | 0.0000  | 0.0000  | 0.0000  | 0.0000  |
| TiO <sub>2</sub>               | 0.0003  | 0.0003 | 0.0003 | 0.0003  | 0.0003  | 0.0003  | 0.0003  | 0.0003  | 0.0003  | 0.0003  | 0.0003  | 0.0003  |
| U <sub>3</sub> O <sub>8</sub>  | 0.0000  | 0.0000 | 0.0000 | 0.0000  | 0.0000  | 0.0000  | 0.0000  | 0.0000  | 0.0000  | 0.0000  | 0.0000  | 0.0000  |
| ZnO                            | 0.0004  | 0.0004 | 0.0004 | 0.0004  | 0.0004  | 0.0004  | 0.0004  | 0.0004  | 0.0004  | 0.0004  | 0.0004  | 0.0004  |
| ZrO <sub>2</sub>               | 0.0179  | 0.0182 | 0.0178 | 0.0185  | 0.0182  | 0.0184  | 0.0182  | 0.0175  | 0.0185  | 0.0183  | 0.0178  | 0.0193  |
| Others                         | 0.0216  | 0.0218 | 0.0214 | 0.0222  | 0.0219  | 0.0262  | 0.0360  | 0.0753  | 0.0223  | 0.0221  | 0.0214  | 0.0232  |

| Component                      | Glass   |         |         |         |         |         |         |         |         |              |         |         |
|--------------------------------|---------|---------|---------|---------|---------|---------|---------|---------|---------|--------------|---------|---------|
|                                | SP-Na-3 | SP-Ni-1 | SP-Ni-2 | SP-Ni-3 | SP-Si-1 | SP-Ti-1 | SP-Zr-1 | Sp-Ru-1 | Sp-Ru-2 | SP-Ot-hers-1 | Sp-LHLL | Sp-LHLH |
| Al <sub>2</sub> O <sub>3</sub> | 0.0759  | 0.0804  | 0.0796  | 0.0780  | 0.0919  | 0.0780  | 0.0782  | 0.0800  | 0.0799  | 0.0777       | 0.0500  | 0.0500  |
| B <sub>2</sub> O <sub>3</sub>  | 0.0665  | 0.0704  | 0.0697  | 0.0683  | 0.0804  | 0.0683  | 0.0685  | 0.0700  | 0.0699  | 0.0680       | 0.0706  | 0.0688  |
| Bi <sub>2</sub> O <sub>3</sub> | 0.0000  | 0.0000  | 0.0000  | 0.0000  | 0.0000  | 0.0000  | 0.0000  | 0.0000  | 0.0000  | 0.0000       | 0.0000  | 0.0000  |
| CaO                            | 0.0095  | 0.0101  | 0.0100  | 0.0098  | 0.0115  | 0.0098  | 0.0098  | 0.0000  | 0.0000  | 0.0097       | 0.0000  | 0.0000  |
| CdO                            | 0.0066  | 0.0070  | 0.0069  | 0.0068  | 0.0080  | 0.0068  | 0.0068  | 0.0088  | 0.0088  | 0.0127       | 0.0089  | 0.0087  |
| Cr <sub>2</sub> O <sub>3</sub> | 0.0021  | 0.0022  | 0.0022  | 0.0021  | 0.0025  | 0.0021  | 0.0022  | 0.0022  | 0.0022  | 0.0021       | 0.0005  | 0.0005  |
| F                              | 0.0006  | 0.0006  | 0.0006  | 0.0006  | 0.0007  | 0.0006  | 0.0006  | 0.0008  | 0.0008  | 0.0011       | 0.0008  | 0.0008  |
| Fe <sub>2</sub> O <sub>3</sub> | 0.1187  | 0.1257  | 0.1244  | 0.1219  | 0.1435  | 0.1219  | 0.1223  | 0.1249  | 0.1249  | 0.1215       | 0.1260  | 0.1228  |
| K <sub>2</sub> O               | 0.0027  | 0.0028  | 0.0028  | 0.0027  | 0.0032  | 0.0027  | 0.0027  | 0.0000  | 0.0000  | 0.0027       | 0.0000  | 0.0000  |
| Li <sub>2</sub> O              | 0.0285  | 0.0302  | 0.0299  | 0.0293  | 0.0344  | 0.0293  | 0.0293  | 0.0300  | 0.0300  | 0.0292       | 0.0302  | 0.0295  |
| MnO                            | 0.0034  | 0.0036  | 0.0036  | 0.0035  | 0.0041  | 0.0035  | 0.0036  | 0.0036  | 0.0036  | 0.0067       | 0.0036  | 0.0035  |
| Na <sub>2</sub> O              | 0.2000  | 0.1581  | 0.1565  | 0.1534  | 0.1806  | 0.1534  | 0.1539  | 0.1572  | 0.1572  | 0.1529       | 0.1873  | 0.1873  |
| NiO                            | 0.0049  | 0.0000  | 0.0100  | 0.0300  | 0.0060  | 0.0051  | 0.0051  | 0.0052  | 0.0052  | 0.0051       | 0.0010  | 0.0200  |
| P <sub>2</sub> O <sub>5</sub>  | 0.0044  | 0.0047  | 0.0046  | 0.0045  | 0.0053  | 0.0045  | 0.0045  | 0.0059  | 0.0059  | 0.0085       | 0.0059  | 0.0058  |
| SiO <sub>2</sub>               | 0.4367  | 0.4624  | 0.4578  | 0.4485  | 0.3800  | 0.4486  | 0.4499  | 0.4597  | 0.4596  | 0.4470       | 0.4636  | 0.4520  |
| SrO                            | 0.0003  | 0.0003  | 0.0003  | 0.0003  | 0.0003  | 0.0003  | 0.0003  | 0.0004  | 0.0004  | 0.0006       | 0.0004  | 0.0004  |
| ThO <sub>2</sub>               | 0.0000  | 0.0000  | 0.0000  | 0.0000  | 0.0000  | 0.0000  | 0.0000  | 0.0000  | 0.0000  | 0.0000       | 0.0000  | 0.0000  |
| TiO <sub>2</sub>               | 0.0003  | 0.0003  | 0.0003  | 0.0003  | 0.0003  | 0.0250  | 0.0003  | 0.0003  | 0.0003  | 0.0003       | 0.0003  | 0.0003  |
| U <sub>3</sub> O <sub>8</sub>  | 0.0000  | 0.0000  | 0.0000  | 0.0000  | 0.0000  | 0.0000  | 0.0000  | 0.0000  | 0.0000  | 0.0000       | 0.0000  | 0.0000  |
| ZnO                            | 0.0004  | 0.0004  | 0.0004  | 0.0004  | 0.0005  | 0.0004  | 0.0004  | 0.0005  | 0.0005  | 0.0007       | 0.0005  | 0.0005  |
| ZrO <sub>2</sub>               | 0.0175  | 0.0186  | 0.0184  | 0.0180  | 0.0212  | 0.0180  | 0.0400  | 0.0234  | 0.0234  | 0.0180       | 0.0236  | 0.0231  |
| Others                         | 0.0211  | 0.0223  | 0.0221  | 0.0217  | 0.0255  | 0.0216  | 0.0217  | 0.0271  | 0.0274  | 0.0355       | 0.0268  | 0.0261  |

Table B.1. Un-normalized 22-Component Mass-Fraction Compositions of the 144 Existing Database Glasses in the Spinel Primary Phase Field Chosen for Augmentation (cont.)

| Component                      | Glass   |         |         |         |         |         |         |         |         |         |         |               |
|--------------------------------|---------|---------|---------|---------|---------|---------|---------|---------|---------|---------|---------|---------------|
|                                | Sp-LHHL | Sp-LHHH | Sp-LHMM | Sp-MMLL | Sp-MMLH | Sp-MMHL | Sp-MMHH | Sp-MMMM | Sp-LHLH | Sp-MMLL | Sp-MMHH | T51-Opt. Frit |
| Al <sub>2</sub> O <sub>3</sub> | 0.0500  | 0.0500  | 0.0500  | 0.0800  | 0.0800  | 0.0800  | 0.0800  | 0.0800  | 0.0500  | 0.0800  | 0.0800  | 0.0628        |
| B <sub>2</sub> O <sub>3</sub>  | 0.0700  | 0.0683  | 0.0700  | 0.0706  | 0.0688  | 0.0700  | 0.0683  | 0.0700  | 0.0688  | 0.0706  | 0.0683  | 0.0508        |
| Bi <sub>2</sub> O <sub>3</sub> | 0.0000  | 0.0000  | 0.0000  | 0.0000  | 0.0000  | 0.0000  | 0.0000  | 0.0000  | 0.0000  | 0.0000  | 0.0000  | 0.0000        |
| CaO                            | 0.0000  | 0.0000  | 0.0000  | 0.0000  | 0.0000  | 0.0000  | 0.0000  | 0.0000  | 0.0000  | 0.0000  | 0.0000  | 0.0186        |
| CdO                            | 0.0088  | 0.0086  | 0.0088  | 0.0089  | 0.0087  | 0.0088  | 0.0086  | 0.0088  | 0.0087  | 0.0089  | 0.0086  | 0.0000        |
| Cr <sub>2</sub> O <sub>3</sub> | 0.0060  | 0.0060  | 0.0022  | 0.0005  | 0.0005  | 0.0060  | 0.0060  | 0.0022  | 0.0005  | 0.0005  | 0.0060  | 0.0012        |
| F                              | 0.0008  | 0.0007  | 0.0008  | 0.0008  | 0.0008  | 0.0008  | 0.0007  | 0.0008  | 0.0008  | 0.0008  | 0.0007  | 0.0000        |
| Fe <sub>2</sub> O <sub>3</sub> | 0.1251  | 0.1219  | 0.1250  | 0.1260  | 0.1228  | 0.1251  | 0.1219  | 0.1250  | 0.1228  | 0.1260  | 0.1219  | 0.2024        |
| K <sub>2</sub> O               | 0.0000  | 0.0000  | 0.0000  | 0.0000  | 0.0000  | 0.0000  | 0.0000  | 0.0000  | 0.0000  | 0.0000  | 0.0000  | 0.0006        |
| Li <sub>2</sub> O              | 0.0300  | 0.0293  | 0.0300  | 0.0302  | 0.0295  | 0.0300  | 0.0293  | 0.0300  | 0.0295  | 0.0302  | 0.0293  | 0.0108        |
| MnO                            | 0.0036  | 0.0035  | 0.0036  | 0.0036  | 0.0035  | 0.0036  | 0.0035  | 0.0036  | 0.0035  | 0.0036  | 0.0035  | 0.0191        |
| Na <sub>2</sub> O              | 0.1873  | 0.1873  | 0.1873  | 0.1573  | 0.1573  | 0.1573  | 0.1573  | 0.1573  | 0.1873  | 0.1573  | 0.1573  | 0.1827        |
| NiO                            | 0.0010  | 0.0200  | 0.0052  | 0.0010  | 0.0200  | 0.0010  | 0.0200  | 0.0052  | 0.0200  | 0.0010  | 0.0200  | 0.0018        |
| P <sub>2</sub> O <sub>5</sub>  | 0.0059  | 0.0058  | 0.0059  | 0.0059  | 0.0058  | 0.0059  | 0.0058  | 0.0059  | 0.0058  | 0.0059  | 0.0058  | 0.0070        |
| SiO <sub>2</sub>               | 0.4602  | 0.4487  | 0.4600  | 0.4636  | 0.4520  | 0.4602  | 0.4487  | 0.4600  | 0.4520  | 0.4636  | 0.4487  | 0.4276        |
| SrO                            | 0.0004  | 0.0004  | 0.0004  | 0.0004  | 0.0004  | 0.0004  | 0.0004  | 0.0004  | 0.0004  | 0.0004  | 0.0004  | 0.0001        |
| ThO <sub>2</sub>               | 0.0000  | 0.0000  | 0.0000  | 0.0000  | 0.0000  | 0.0000  | 0.0000  | 0.0000  | 0.0000  | 0.0000  | 0.0000  | 0.0000        |
| TiO <sub>2</sub>               | 0.0003  | 0.0003  | 0.0003  | 0.0003  | 0.0003  | 0.0003  | 0.0003  | 0.0003  | 0.0003  | 0.0003  | 0.0003  | 0.0003        |
| U <sub>3</sub> O <sub>8</sub>  | 0.0000  | 0.0000  | 0.0000  | 0.0000  | 0.0000  | 0.0000  | 0.0000  | 0.0000  | 0.0000  | 0.0000  | 0.0000  | 0.0000        |
| ZnO                            | 0.0005  | 0.0005  | 0.0005  | 0.0005  | 0.0005  | 0.0005  | 0.0005  | 0.0005  | 0.0005  | 0.0005  | 0.0005  | 0.0009        |
| ZrO <sub>2</sub>               | 0.0234  | 0.0229  | 0.0234  | 0.0236  | 0.0231  | 0.0234  | 0.0229  | 0.0234  | 0.0231  | 0.0236  | 0.0229  | 0.0000        |
| Others                         | 0.0265  | 0.0259  | 0.0265  | 0.0268  | 0.0261  | 0.0265  | 0.0259  | 0.0265  | 0.0261  | 0.0268  | 0.0259  | 0.0133        |

| Component                      | Glass     |           |          |          |          |           |           |           |            |           |           |           |
|--------------------------------|-----------|-----------|----------|----------|----------|-----------|-----------|-----------|------------|-----------|-----------|-----------|
|                                | LSi-Al-13 | LSi-Al-16 | LSi-B-09 | LSi-B-12 | LSi-Fe-2 | LSi-Mn-03 | LSi-Na-16 | LSi-Na-19 | LSi-Ni-025 | LSi-Si-39 | LSi-Si-42 | LSi-Zr-05 |
| Al <sub>2</sub> O <sub>3</sub> | 0.1300    | 0.1600    | 0.0968   | 0.0936   | 0.0936   | 0.0982    | 0.1083    | 0.1045    | 0.0984     | 0.0958    | 0.0911    | 0.0969    |
| B <sub>2</sub> O <sub>3</sub>  | 0.0580    | 0.0560    | 0.0900   | 0.1200   | 0.0562   | 0.0589    | 0.0650    | 0.0627    | 0.0590     | 0.0575    | 0.0547    | 0.0582    |
| Bi <sub>2</sub> O <sub>3</sub> | 0.0000    | 0.0000    | 0.0000   | 0.0000   | 0.0000   | 0.0000    | 0.0000    | 0.0000    | 0.0000     | 0.0000    | 0.0000    | 0.0000    |
| CaO                            | 0.0010    | 0.0010    | 0.0010   | 0.0010   | 0.0010   | 0.0010    | 0.0011    | 0.0011    | 0.0010     | 0.0010    | 0.0010    | 0.0010    |
| CdO                            | 0.0159    | 0.0153    | 0.0159   | 0.0154   | 0.0154   | 0.0162    | 0.0179    | 0.0172    | 0.0162     | 0.0158    | 0.0150    | 0.0160    |
| Cr <sub>2</sub> O <sub>3</sub> | 0.0013    | 0.0012    | 0.0013   | 0.0012   | 0.0012   | 0.0013    | 0.0014    | 0.0014    | 0.0013     | 0.0013    | 0.0012    | 0.0013    |
| F                              | 0.0001    | 0.0001    | 0.0001   | 0.0001   | 0.0001   | 0.0001    | 0.0001    | 0.0001    | 0.0001     | 0.0001    | 0.0001    | 0.0001    |
| Fe <sub>2</sub> O <sub>3</sub> | 0.1404    | 0.1356    | 0.1407   | 0.1360   | 0.2000   | 0.1427    | 0.1575    | 0.1518    | 0.1430     | 0.1393    | 0.1324    | 0.1408    |
| K <sub>2</sub> O               | 0.0003    | 0.0003    | 0.0003   | 0.0003   | 0.0003   | 0.0003    | 0.0003    | 0.0003    | 0.0003     | 0.0003    | 0.0003    | 0.0003    |
| Li <sub>2</sub> O              | 0.0145    | 0.0140    | 0.0145   | 0.0140   | 0.0140   | 0.0147    | 0.0163    | 0.0157    | 0.0148     | 0.0144    | 0.0137    | 0.0145    |
| MnO                            | 0.0120    | 0.0116    | 0.0120   | 0.0116   | 0.0116   | 0.0300    | 0.0134    | 0.0130    | 0.0122     | 0.0119    | 0.0113    | 0.0120    |
| Na <sub>2</sub> O              | 0.2175    | 0.2100    | 0.2178   | 0.2106   | 0.2106   | 0.2210    | 0.1600    | 0.1900    | 0.2214     | 0.2156    | 0.2050    | 0.2181    |
| NiO                            | 0.0090    | 0.0087    | 0.0090   | 0.0087   | 0.0087   | 0.0091    | 0.0101    | 0.0097    | 0.0250     | 0.0089    | 0.0085    | 0.0090    |
| P <sub>2</sub> O <sub>5</sub>  | 0.0029    | 0.0028    | 0.0029   | 0.0028   | 0.0028   | 0.0029    | 0.0032    | 0.0031    | 0.0029     | 0.0029    | 0.0027    | 0.0029    |
| SiO <sub>2</sub>               | 0.3515    | 0.3394    | 0.3520   | 0.3404   | 0.3403   | 0.3571    | 0.3941    | 0.3800    | 0.3579     | 0.3900    | 0.4200    | 0.3525    |
| SrO                            | 0.0172    | 0.0166    | 0.0172   | 0.0167   | 0.0167   | 0.0175    | 0.0193    | 0.0186    | 0.0175     | 0.0171    | 0.0162    | 0.0173    |
| ThO <sub>2</sub>               | 0.0000    | 0.0000    | 0.0000   | 0.0000   | 0.0000   | 0.0000    | 0.0000    | 0.0000    | 0.0000     | 0.0000    | 0.0000    | 0.0000    |
| TiO <sub>2</sub>               | 0.0001    | 0.0001    | 0.0001   | 0.0001   | 0.0001   | 0.0001    | 0.0001    | 0.0001    | 0.0001     | 0.0001    | 0.0001    | 0.0001    |
| U <sub>3</sub> O <sub>8</sub>  | 0.0000    | 0.0000    | 0.0000   | 0.0000   | 0.0000   | 0.0000    | 0.0000    | 0.0000    | 0.0000     | 0.0000    | 0.0000    | 0.0000    |
| ZnO                            | 0.0005    | 0.0005    | 0.0005   | 0.0005   | 0.0005   | 0.0005    | 0.0006    | 0.0006    | 0.0005     | 0.0005    | 0.0005    | 0.0005    |
| ZrO <sub>2</sub>               | 0.0193    | 0.0186    | 0.0193   | 0.0187   | 0.0187   | 0.0196    | 0.0216    | 0.0208    | 0.0196     | 0.0191    | 0.0182    | 0.0500    |
| Others                         | 0.0085    | 0.0082    | 0.0085   | 0.0082   | 0.0082   | 0.0086    | 0.0095    | 0.0092    | 0.0086     | 0.0084    | 0.0080    | 0.0085    |

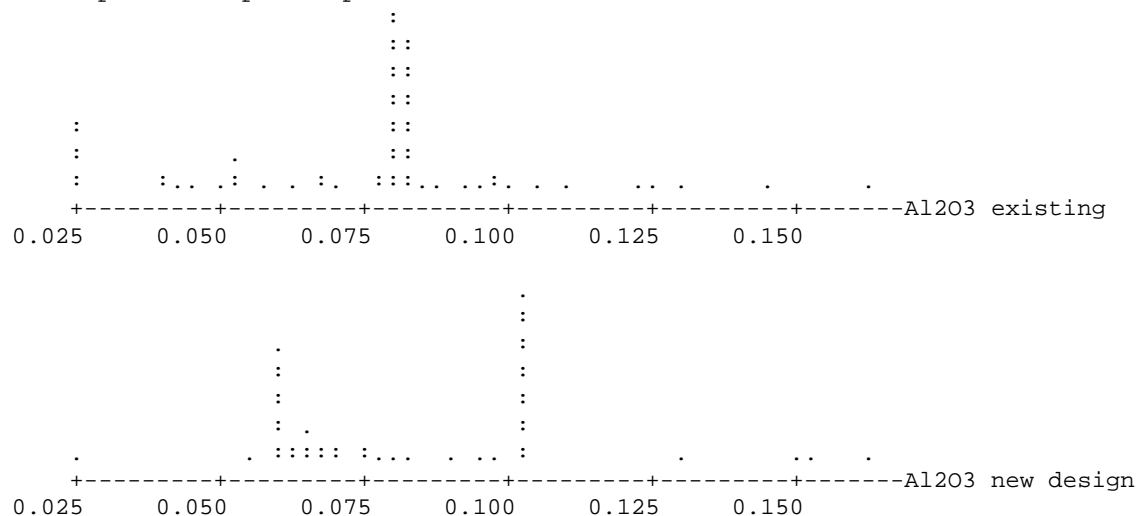
## **Appendix C**

### **Dot Plots for Existing Glasses and New Experimental Design Glasses**

Appendix C shows dot plots of the normalized 21-components for the 144 existing glasses and the 45 new experimental design glasses. Figure C.1 contains several dot plots, one for each component, listed in alphabetical order.

## Dotplot: Al2O3

Each dot represents up to 3 points



## Dotplot: B2O3

Each dot represents up to 2 points

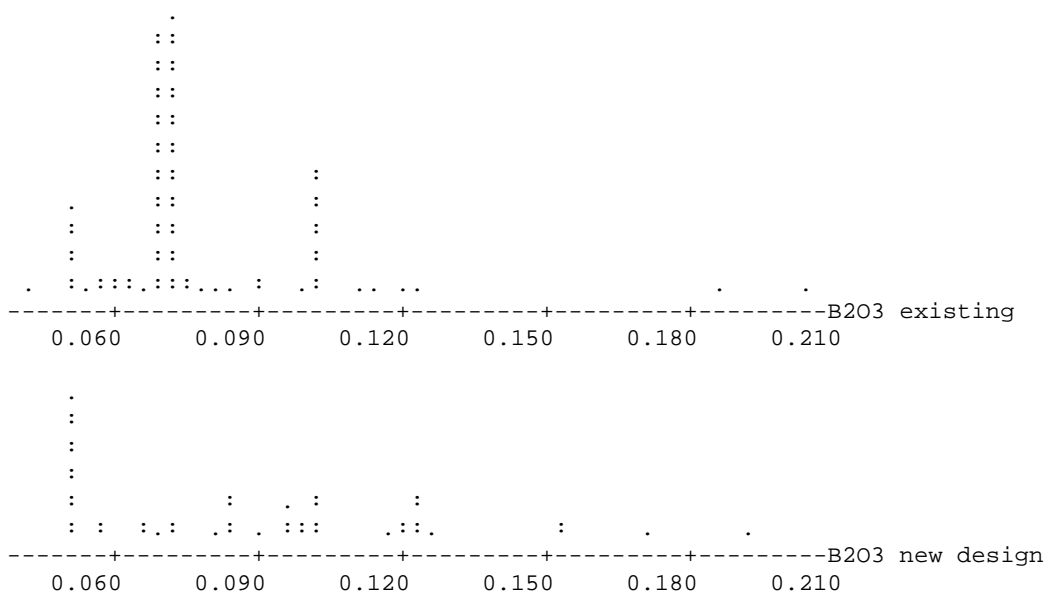
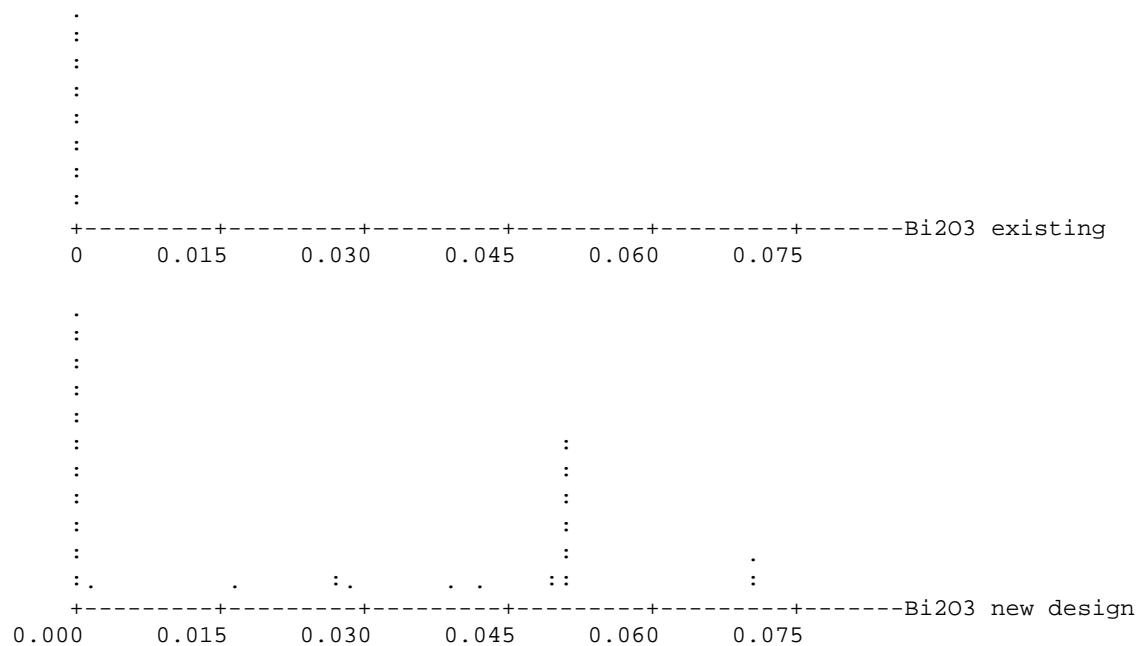


Figure C.1. Dot Plots of 21-Component Normalized Mass Fractions for 144 Existing Spinel Glasses and 45 New Experimental Design Glasses



### Dotplot: Bi2O3

Each dot represents up to 10 points



### Dotplot: CaO

Each dot represents up to 3 points

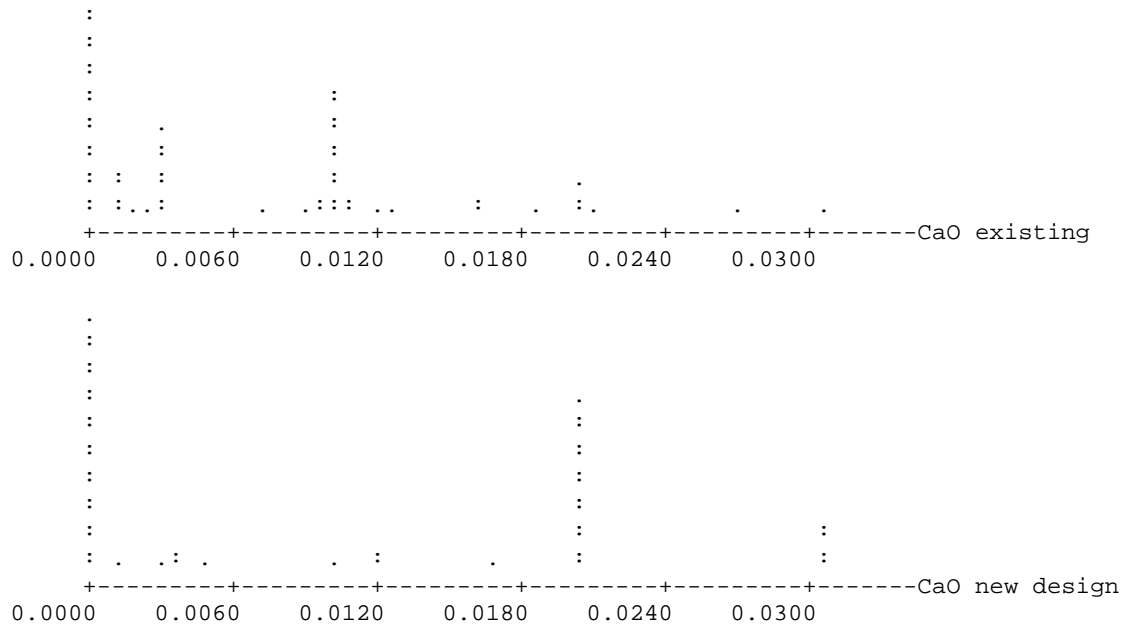
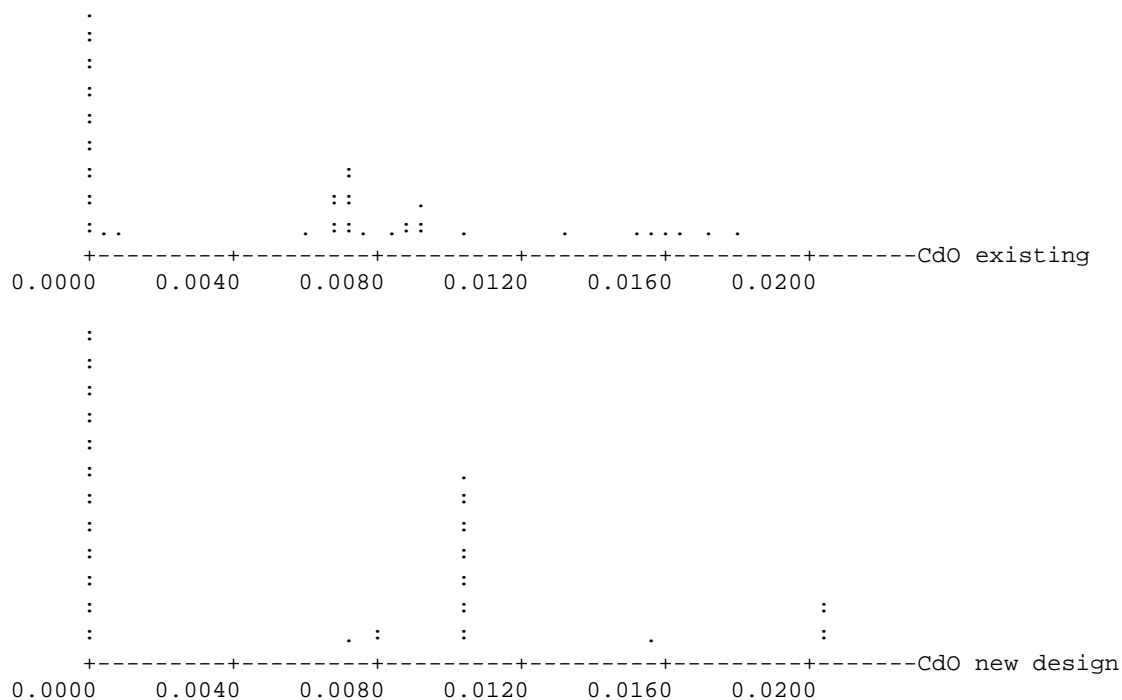


Figure C.1. Dot Plots of 21-Component Normalized Mass Fractions for 144 Existing Spinel Glasses and 45 New Experimental Design Glasses (cont.)

### Dotplot: CdO

Each dot represents up to 4 points



### Dotplot: Cr2O3

Each dot represents up to 2 points

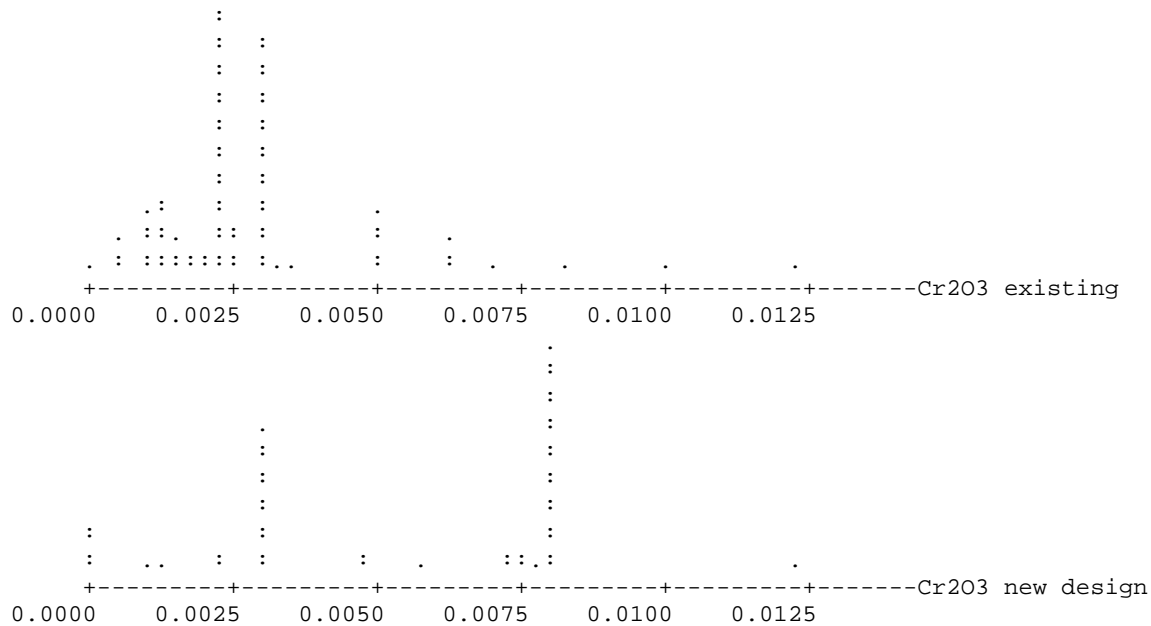
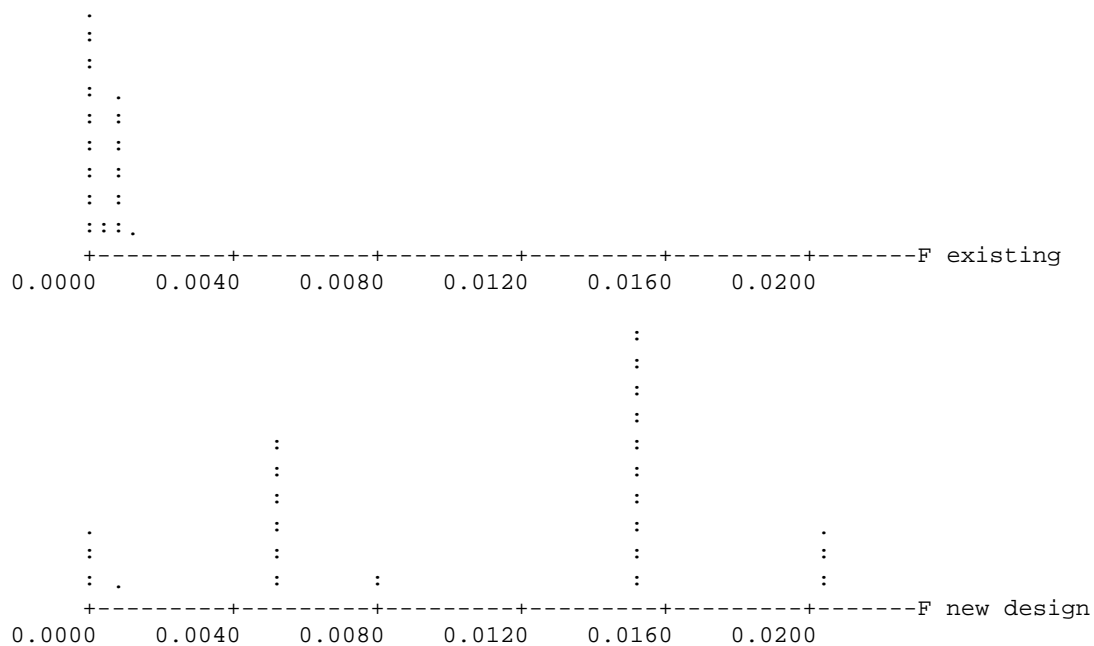


Figure C.1. Dot Plots of 21-Component Normalized Mass Fractions for 144 Existing Spinel Glasses and 45 New Experimental Glasses (cont.)

### Dotplot: F

Each dot represents up to 5 points



### Dotplot: Fe2O3

Each dot represents up to 2 points

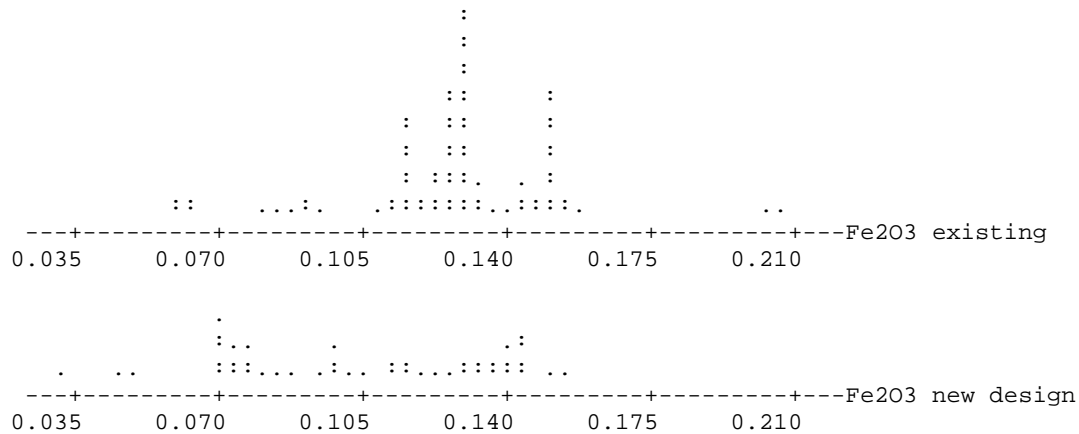
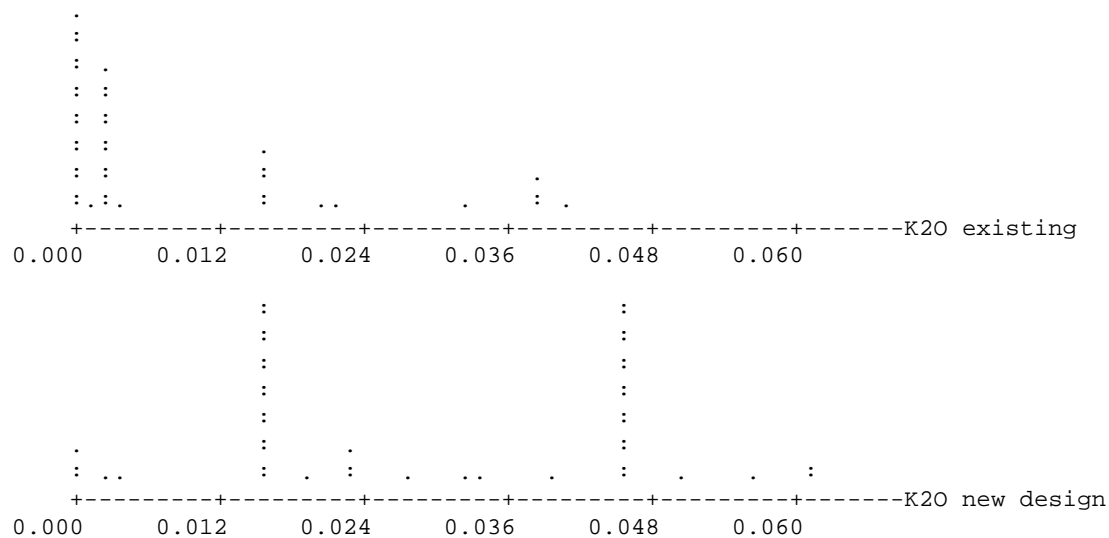


Figure C.1. Dot Plots of 21-Component Normalized Mass Fractions for 144 Existing Spinel Glasses and 45 New Experimental Design Glasses (cont.)

## Dotplot: K2O

Each dot represents up to 4 points



## Dotplot: Li2O

Each dot represents up to 2 points

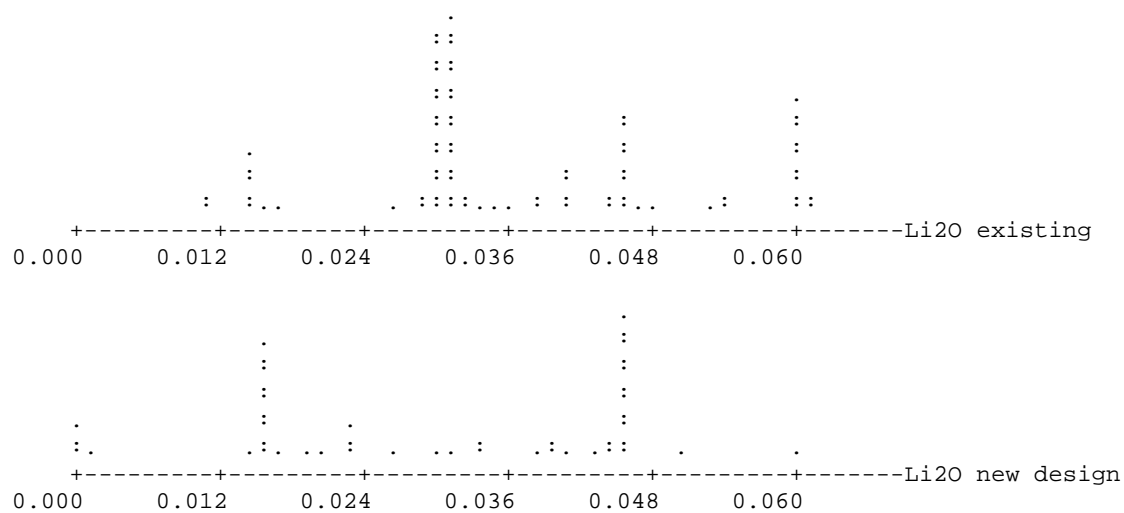
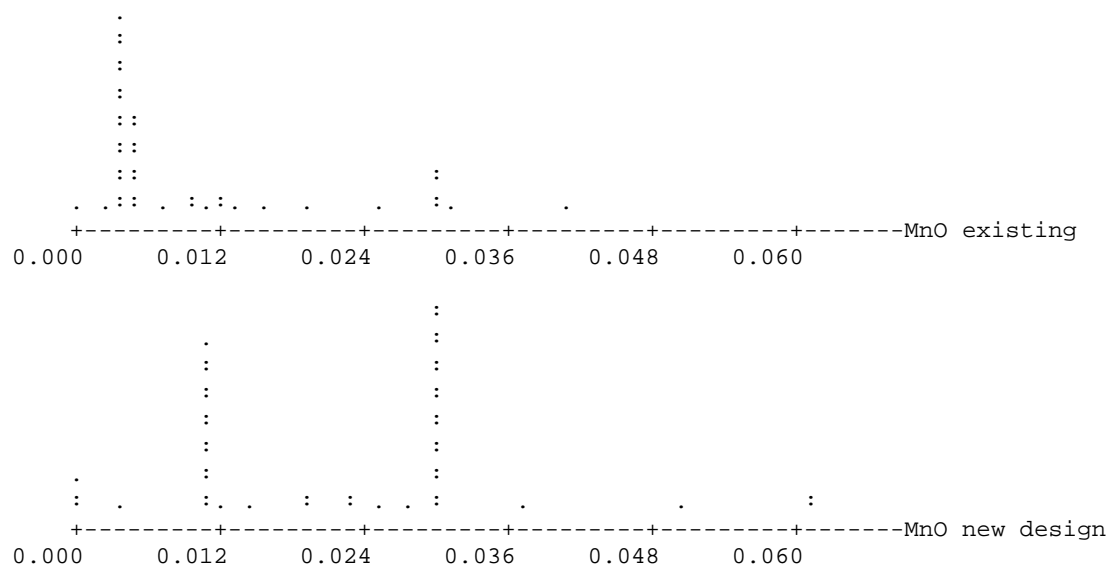


Figure C.1. Dot Plots of 21-Component Normalized Mass Fractions for 144 Existing Spinel Glasses and 45 New Experimental Design Glasses (cont.)

### Dotplot: MnO

Each dot represents up to 4 points



### Dotplot: Na2O

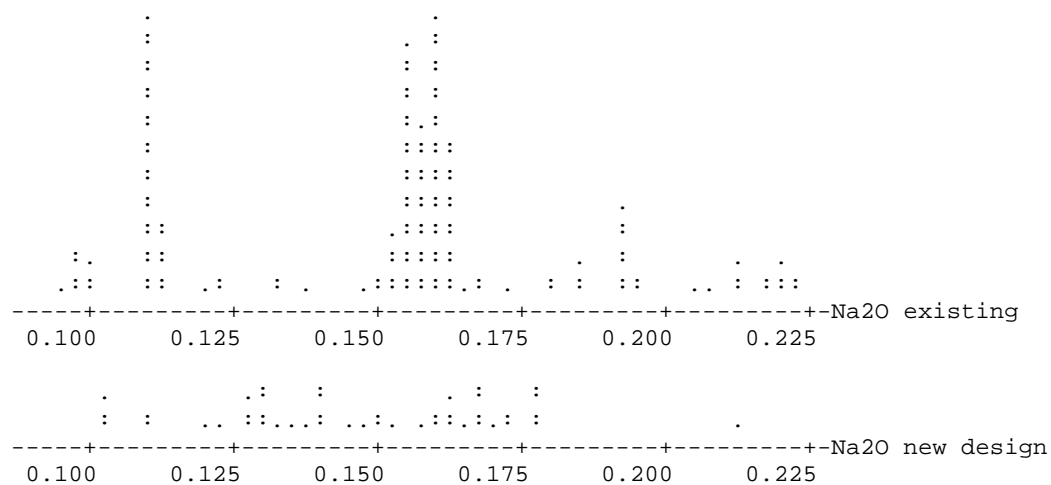
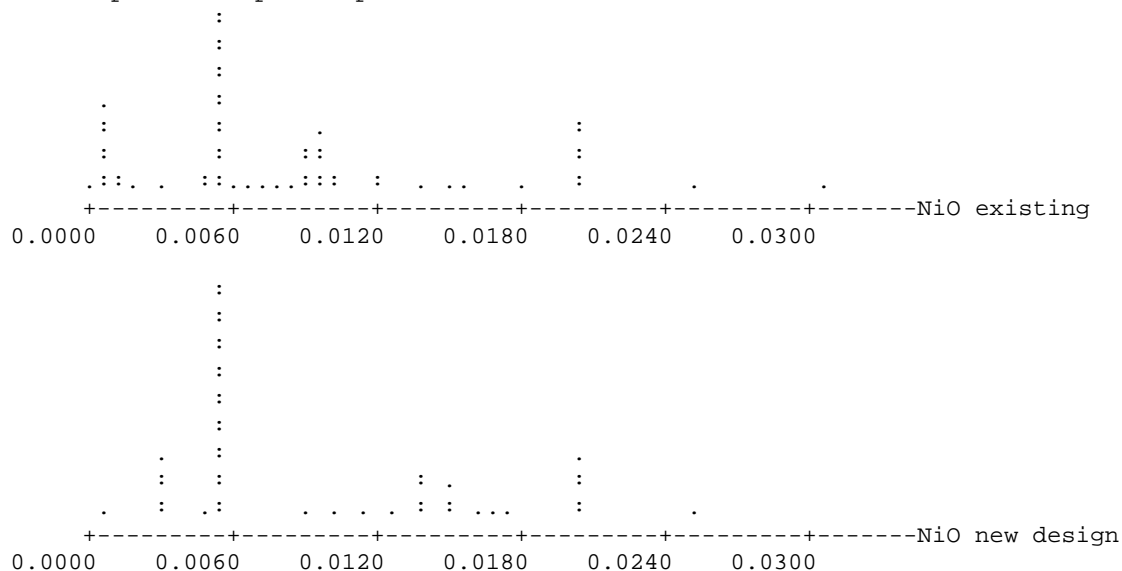


Figure C.1. Dot Plots of 21-Component Normalized Mass Fractions for 144 Existing Spinel Glasses and 45 New Experimental Design Glasses (cont.)

### Dotplot: NiO

Each dot represents up to 3 points



### Dotplot: P2O5

Each dot represents up to 4 points

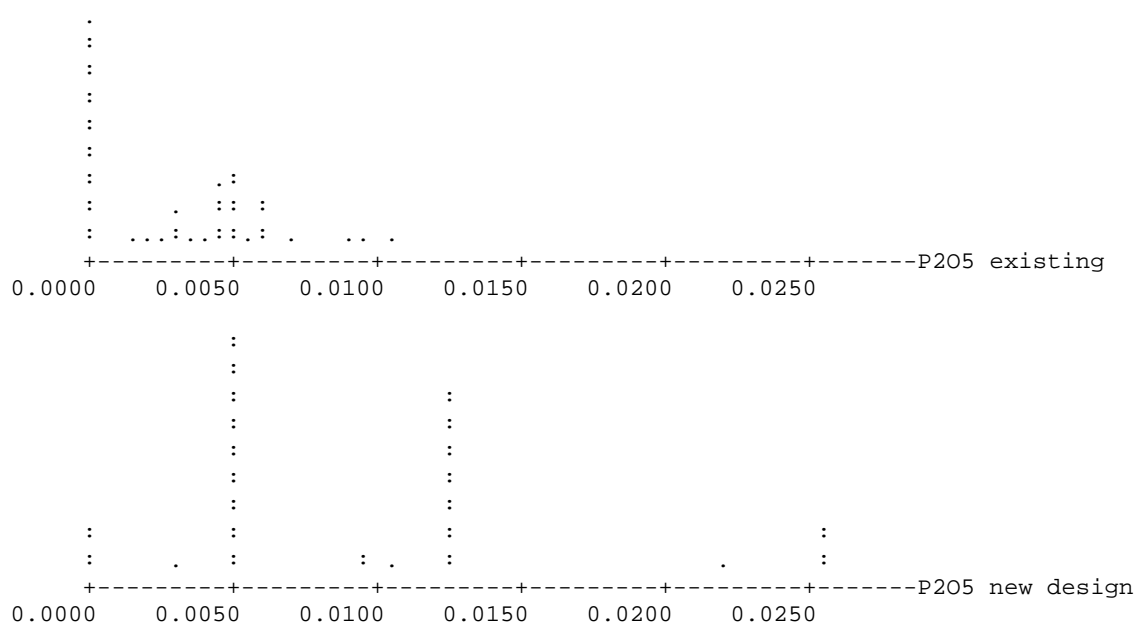
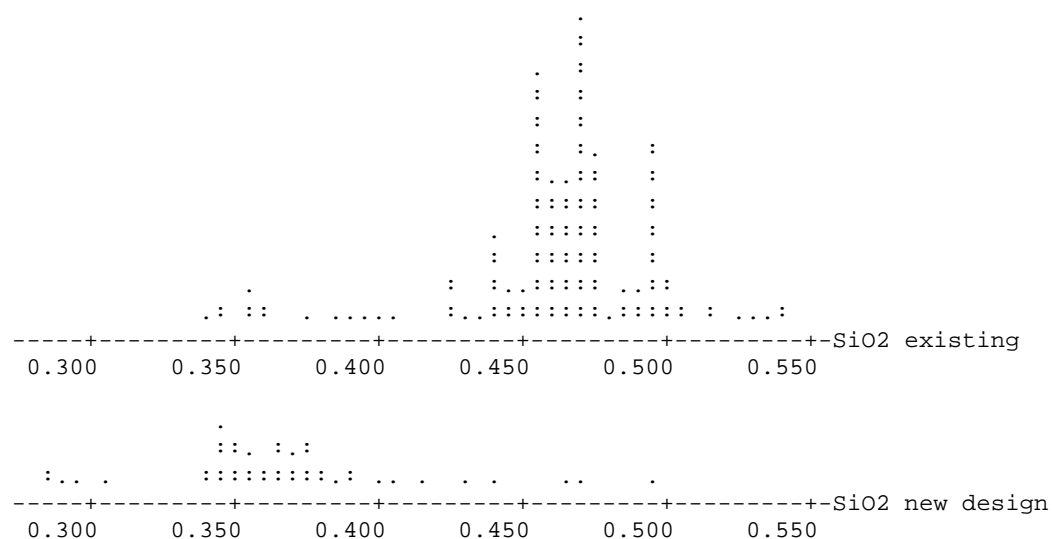


Figure C.1. Dot Plots of 21-Component Normalized Mass Fractions for 144 Existing Spinel Glasses and 45 New Experimental Design Glasses (cont.)

## Dotplot: SiO2



## Dotplot: SrO

Each dot represents up to 9 points

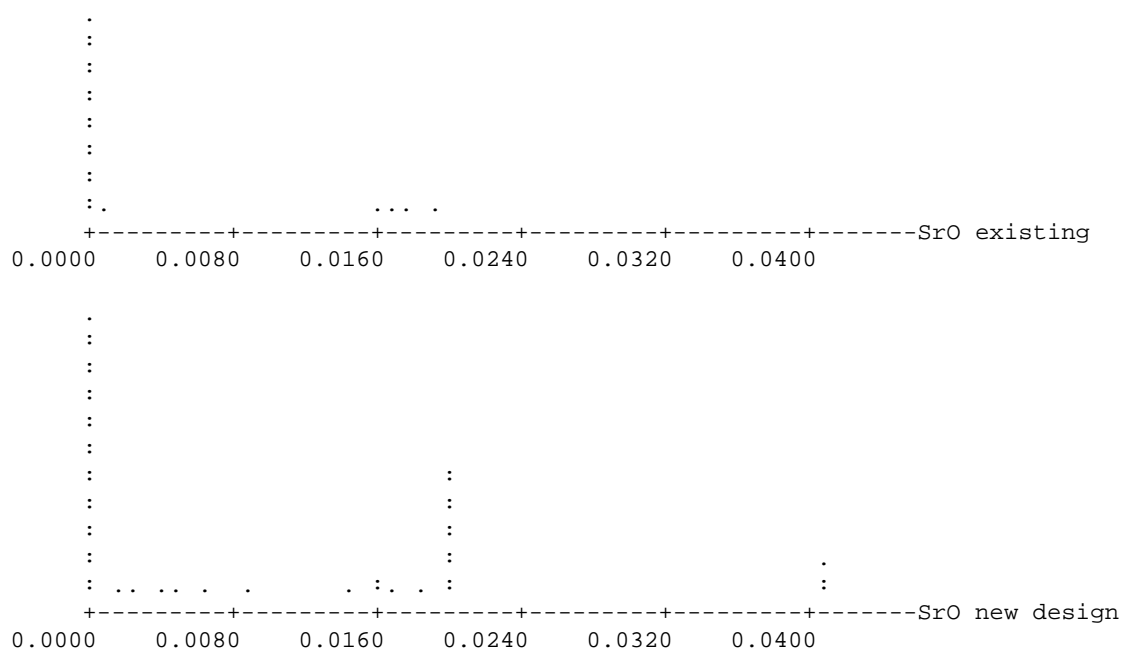
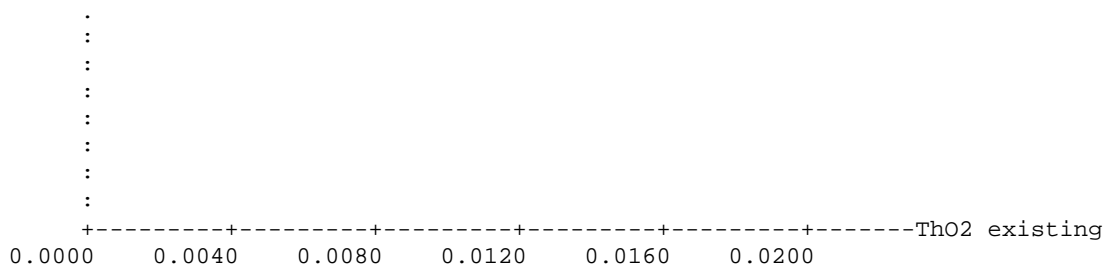


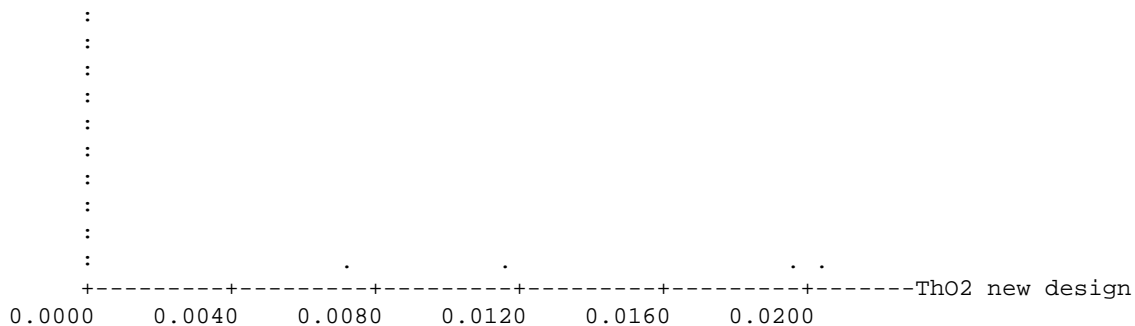
Figure C.1. Dot Plots of 21-Component Normalized Mass Fractions for 144 Existing Spinel Glasses and 45 New Experimental Design Glasses (cont.)

## Dotplot: ThO2

Each dot represents up to 10 points



Each dot represents up to 2 points



## Dotplot: TiO2

Each dot represents up to 4 points

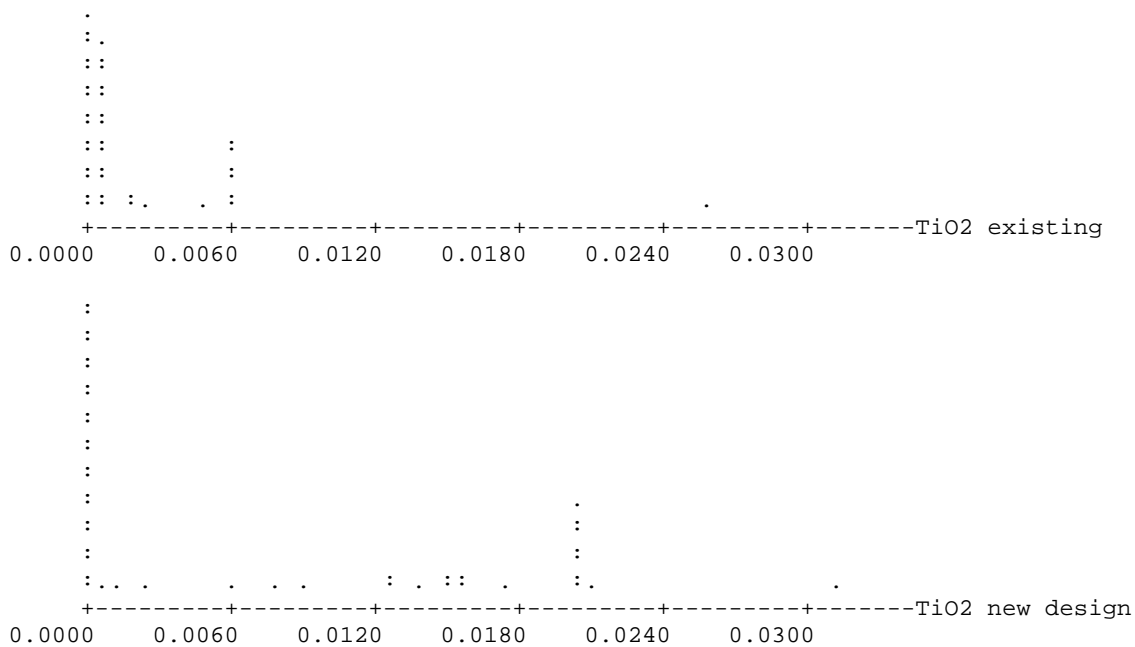
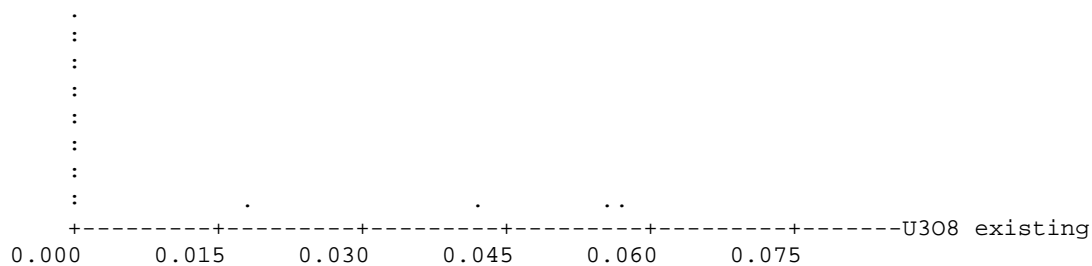


Figure C.1. Dot Plots of 21-Component Normalized Mass Fractions for 144 Existing Spinel Glasses and 45 New Experimental Design Glasses (cont.)

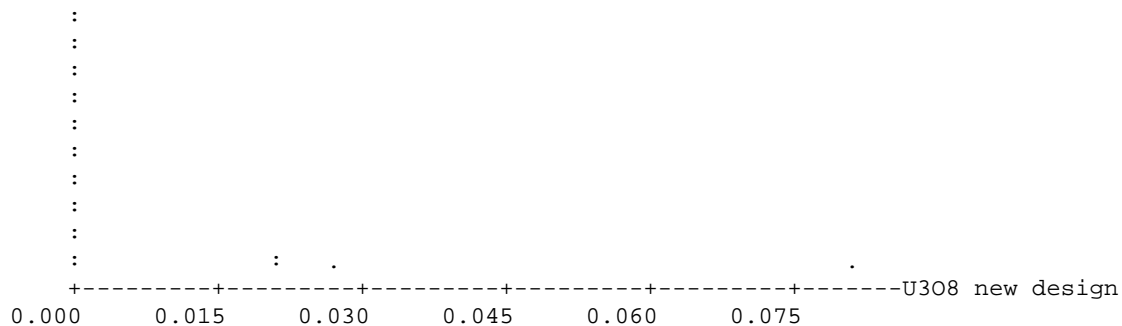


### Dotplot: U3O8

Each dot represents up to 9 points



Each dot represents up to 2 points



### Dotplot: ZnO

Each dot represents up to 5 points

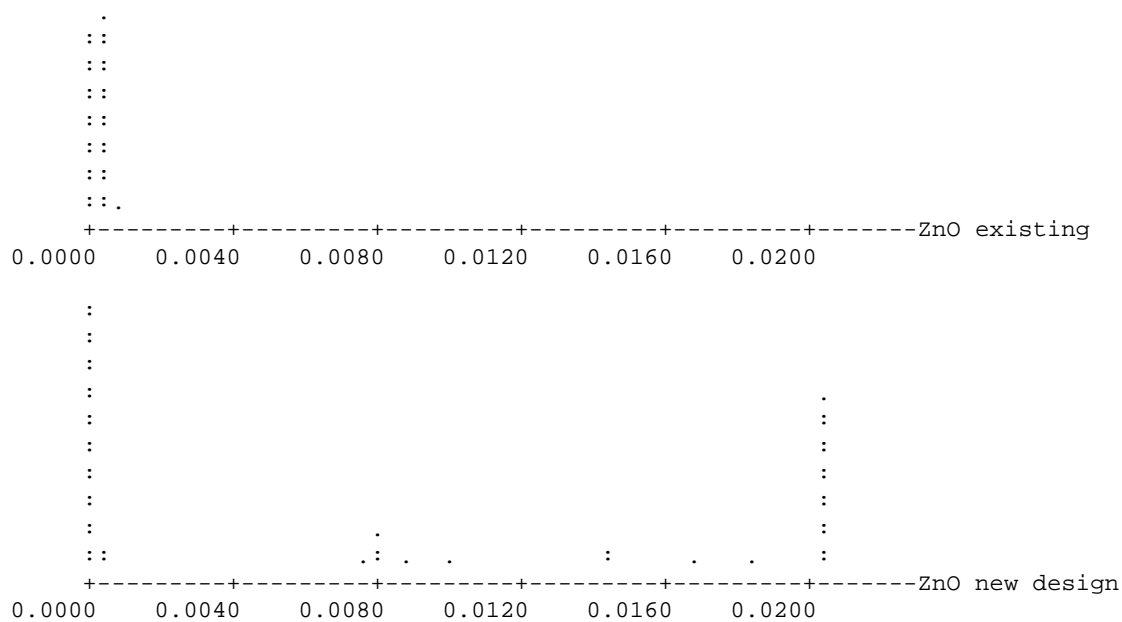


Figure C.1. Dot Plots of 21-Component Normalized Mass Fractions for 144 Existing Spinel Glasses and 45 New Experimental Design Glasses (cont.)

## Dotplot: ZrO2

Each dot represents up to 2 points

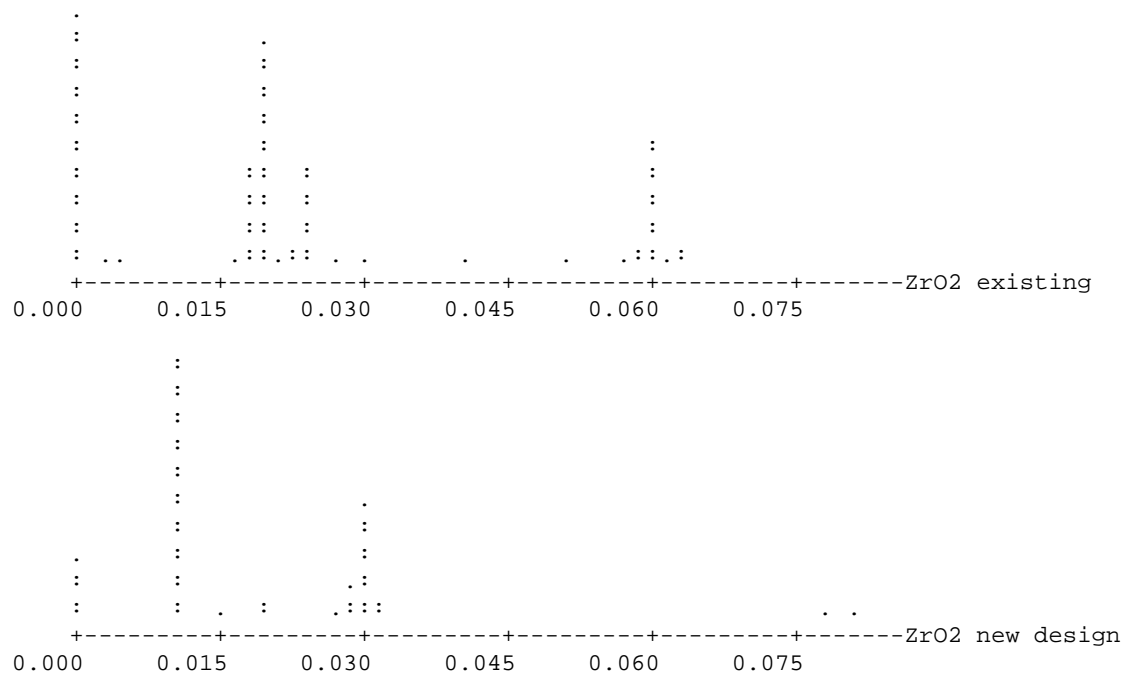


Figure C.1. Dot Plots of 21-Component Normalized Mass Fractions for 144 Existing Spinel Glasses and 45 New Experimental Design Glasses

## Distribution

No. of  
Copies

OFFSITE

Bradley Jones  
JMP, A Business Unit of SAS  
SAS Campus Drive  
Cary, NC 27513

No. of  
Copies

ONSITE

2 **Pacific Northwest National Laboratory**

|           |       |
|-----------|-------|
| GF Piepel | K5-12 |
| SK Cooley | K5-12 |